Design, Synthesis, and Evaluation of γ-Phosphono Diester Analogues of Glutamate as Highly Potent Inhibitors and Active Site Probes of γ-Glutamyl Transpeptidase[†]

Liyou Han, Jun Hiratake,* Akane Kamiyama, and Kanzo Sakata

Institute for Chemical Research, Kyoto University, Uji, Kyoto 611-0011, Japan

Received September 11, 2006; Revised Manuscript Received November 8, 2006

ABSTRACT: γ-Glutamyl transpeptidase (GGT, EC 2.3.2.2) catalyzes the transfer of the γ-glutamyl group of glutathione and related γ-glutamyl amides to water (hydrolysis) or to amino acids and peptides (transpeptidation) and plays a central role in glutathione metabolism. GGT is involved in a number of biological events, such as drug resistance and metastasis of cancer cells by detoxification of xenobiotics and reactive oxygen species through glutathione metabolism, and is also implicated in physiological disorders, such as Parkinson's disease, neurodegerative disease, diabetes, and cardiovascular diseases. In this study, we designed, synthesized, and evaluated a series of γ-phosphono diester analogues of glutamate as transition-state mimic inhibitors of GGT. The electrophilic phosphonate diesters served as highly potent mechanism-based inhibitors that caused the time-dependent and irreversible inhibition of both the *E. coli* and human enzymes, probably by phosphonylating the catalytic Thr residue of the enzyme. In particular, one of the inhibitors exhibited more than 6000 times higher activity toward human GGT than acivicin, a classical but nonselective inhibitor of GGT. The dependence of the inactivation rate on the leaving group ability of the phosphonates (Brønsted plot) revealed that the phosphonylation of the catalytic Thr residue proceeded via a dissociative transition-state with substantial bond cleavage between the phosphorus and the leaving group for both *E. coli* and human GGTs. The binding site of GGT for the Cys−Gly moiety of glutathione or for the acceptor molecules was probed by the phosphonate diesters to reveal a significant difference in the mechanism of substrate recognition between *E. coli* and human GGT. Thus, in the human enzyme, a specific residue in the Cys−Gly binding site played a critical role in recognizing the Cys−Gly moiety or the acceptor molecules by interacting with the C-terminal carboxy group, whereas the Cys side chain and the Cys−Gly amide bond were not recognized significantly. In contrast, the *E. coli* enzyme was a nonselective enzyme that accommodated substrates without specifically recognizing the C-terminal carboxy group of the Cys−Gly moiety of γ-glutamyl compounds or the acceptor molecules. The phosphonate diester-based GGT inhibitors shown here should serve as a blue print for the future design of highly selective GGT inhibitors for use as drug leads and biological probes that gain insight into the hitherto undefined physiological roles of GGT and the relationships between GGT and a variety of diseases.

γ-Glutamyl transpeptidase (GGT,[1] EC 2.3.2.2) is a heterodimeric enzyme found widely in organisms ranging from bacteria to mammals and plays a central role in the metabolism of glutathione and its S-conjugates through the cleavage of the γ-glutamyl amide bond (*1*, *2*). In mammalian cells, GGT is bound to the external surface of the plasma membrane and is expressed in high concentrations in kidney tubules, biliary epithelium, and brain capillaries (*1*−*4*), but in *E. coli*, the enzyme is expressed in periplasmic space as a soluble form (*5*). GGT is believed to play critical roles in cellular cysteine salvage and recovery of other constituent amino acids through the hydrolysis of extracellular glutathione (*3*, *5*−*7*). In mammals, GGT is involved in a number of important physiological processes such as the detoxification of xenobiotics through the cleavage of the γ-glutamyl linkage of glutathione S-conjugates (*1*, *2*, *3*, *8*). Although the detoxification of xenobiotics and the reduction of oxidative stress are highly dependent on cellular glutathione levels, the biosynthesis of glutathione is limited by the availability of cysteine (*3*, *9*). Accordingly, the overexpression of GGT is often observed in human tumors, and its roles in tumor progression (*10*) and the expression of malignant phenotypes of cancer cells, such as drug resistance (*11*−*14*) and metastasis (*15*−*17*), have been suggested repeatedly (*18*). GGT is also implicated in many physiological disorders, such as neurodegenerative diseases (*19*, *20*), diabetes (*21*, *22*), and cardiovascular diseases (*23*, *24*), in connection with oxidative stress and glutathione homeostasis. Therefore, the important roles played by GGT in glutathone-mediated detoxification and cellular response to oxidative stress suggest that GGT is an attractive pharmaceutical target for cancer chemotherapy and a vast array of physiological

[†] This study was supported in part by Grant-in-Aid for Scientific Research from Japan for the Promotion of Science to J.H. (contract no. 16310152).

* To whom correspondence should be addressed. Phone: +81-774-38-3231. Fax: +81-774-38-3229. E-mail: hiratake@scl.kyoto.u-ac.jp.

[1] Abbreviations: GGT, γ-glutamyl transpeptidase; DON, 6-diazo-5-oxo-L-norleucine; APBA, 2-amino-4-phosphonobutanoic acid; Et_3N, triethylamine; γ-Glu-AMC, 7-(γ-L-glutamylamino)-4-methylcoumarin; AMC, 7-amino-4-methylcoumarin; Z, benzyloxycarbonyl; TS, transition state; EDC, 1-(3-dimethylaminopropyl)-3-ethylcarbodiimide hydrochloride.

10.1021/bi061890j CCC: $37.00
Published on Web 01/10/2007

Scheme 1: Proposed Catalytic Mechanism of GGT

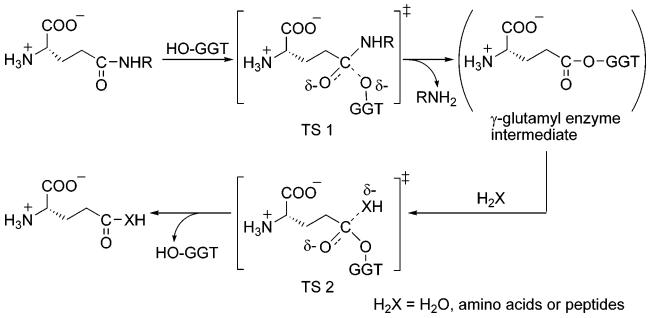

disorders related to oxidative stress and reactive oxygen species.

GGT cleaves the γ-glutamyl bond of glutathione, its S-conjugates, and structurally diverse γ-glutamyl amides to transfer the γ-glutamyl group to water (hydrolysis) or to a variety of amino acids and peptides (transpeptidation) through a modified ping−pong mechanism involving a γ-glutamyl enzyme intermediate (Scheme 1) (*25*, *26*).

Although a number of inhibitors have been reported to date, few compounds appear to serve as potent and specific inhibitors of GGT that could be used *in vivo* as physiological probes and potential drug leads. L-(α*S*,5*S*)-α-Amino-3-chloro-4,5-dihydro-5-isoxazoleacetic acid (acivicin, AT-125), a classical and most widely used irreversible inhibitor of GGT (*27*−*29*), and other glutamine antagonists, such as L-azaserine (*30*, *31*) and 6-diazo-5-oxo-L-norleucine (DON) (*31*), are strong inhibitors of glutamine-dependent amidotransferases (*32*−*35*) and inactivate a number of biosynthetic enzymes for purine and pyrimidine, amino acids, and amino sugars to exert potent cytotoxicity (*34*, *35*). Recently, L-2-amino-4-boronobutanoic acid, a γ-boronic acid analogue of glutamate, was reported to be a slow-binding inhibitor of GGT (*36*, *37*), but the inhibition was reversible, and the inactivated enzyme rapidly regained activity (*36*).

We previously reported that a series of γ-phosphono monoester analogues of glutamate **1a**−**d** served as mechanism-based inhibitors that inactivated GGT by covalent modification of the active site (*38*). The phosphono monoesters gave a stable adduct with the catalytic Thr residue of GGT by mechanism-based phosphonylation (*39*), but their inhibitory activities were relatively low, especially toward human GGT (*38*).

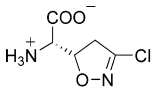

acivicin

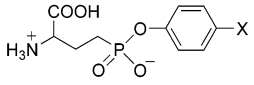

1a : X = H, **1b** : CF_3, **1c** : X = Ac **1d** : CN

This might be due, in part, to the lower electrophilic nature of negatively charged phosphonate monoesters (*40*) or to the lower affinity of the phosphonate monoesters for the enzyme active site by electrostatic repulsion (*41*). Herein we report the design, synthesis, and evaluation of a series of γ-phosphono diester analogues of glutamate **2a**−**g**, **3**, **4**, **5a**, and **5b** as the second generation phosphonate-based inhibitors of GGT. The neutral phosphonate diesters were expected to be chemically more reactive than the monoesters, thus rapidly phosphonylating the catalytic residue to efficiently inactivate GGT (Figure 1). Furthermore, the phosphonate diesters allow

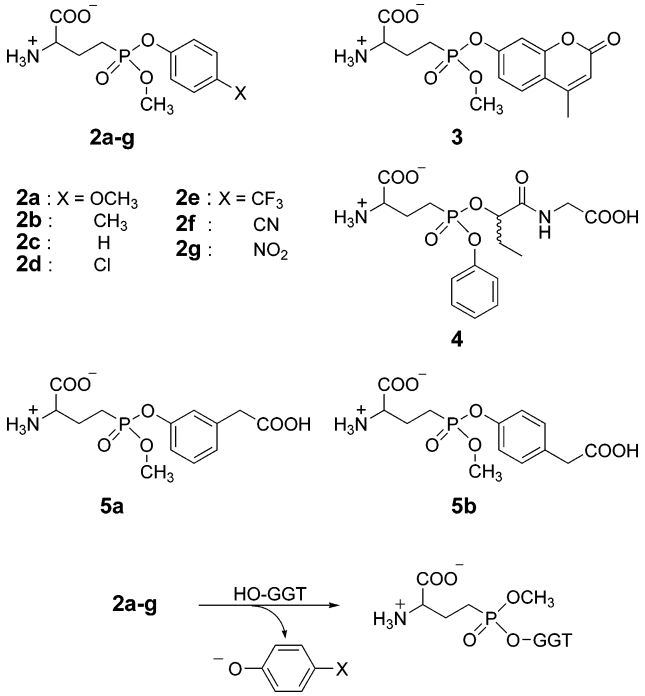

FIGURE 1: Structure of phosphonate diesters **2a**−**g**, **3**, **4**, **5a**, and **5b** and the proposed mechanism of GGT inactivation.

structural elaboration at two sites of the γ-phosphono diester by incorporating a variety of leaving groups (substituted phenols) and a ligand equivalent to the Cys−Gly moiety of glutathione or the acceptor molecules to mimic the transition state for the hydrolysis of glutathione (TS 1) or for the transpeptidation with amino acids (TS 2) (Scheme 1).

The phosphonate diesters **2a**−**g** and **3** served as excellent irreversible inhibitors that caused time-dependent inhibition of both the *E. coli* and human enzymes with rates more than 2 orders of magnitude higher than those of the monoesters **1a**−**d**. In particular, inhibitor **3** exhibited activity toward human GGT ca. 6000 and 20,000 times higher than that of acivicin and monoester **1d**, respectively. The exceptionally high activity of compound **3** toward human GGT inspired the structural elaboration for a series of novel phosphonate diesters **4**, **5a**, and **5b** for use as chemical probes to explore the active-site geometries of *E. coli* and human GGT. This article describes the detailed structure−activity relationships in the inhibition of *E. coli* and human GGT by a series of the phosphonate diesters, a significant difference between the human and bacterial enzymes in active-site structure, and the mechanism of substrate recognition as probed by the inhibitors.

EXPERIMENTAL PROCEDURES

Materials and Methods. Unless otherwise stated, all chemicals were obtained commercially and used without further purification. 7-(γ-L-Glutamylamino)-4-methylcoumarin (γ-Glu-AMC) was purchased from Sigma. Racemic 2-amino-4-phosphonobutanoic acid (APBA) was synthesized as described in the literature (*42*, *43*). Dry CH_2Cl_2 and dry triethylamine (Et_3N) were prepared by distillation from CaH_2 and stored over Molecular Sieves 4Å. *E. coli* γ-glutamyl transpeptidase was purified from the periplasmic fraction of a recombinant strain of *E. coli* K-12 (SH642) as described previously (*5*). Human γ-glutamyl transpeptidase HC-GTP

(T-72) was a generous gift from Asahi Kasei Corporation (Osaka, Japan). The latter enzyme preparation contained a large amount of bovine serum albumin (BSA) as the enzyme stabilizer (GGT content <1%).

The protein concentration was determined by Bradford's method with BSA as a standard (*45*). ^{1}H and ^{31}P NMR spectra were recorded on a JEOL JNM-AL 300 (300 MHz for ^{1}H). Chemical shifts were recorded relative to the internal standard (tetramethylsilane for ^{1}H) or to the external standard (sodium 3-(trimethylsilyl)propanesulfonate for ^{1}H in D_2O and 85% H_3PO_4 for ^{31}P). Infrared spectra were recorded on a HORIBA FT-720 infrared spectrophotometer. Mass spectra were obtained on a JEOL JMS 700 spectrometer. Elemental analyses were performed on a Yanaco MT-5. Thin layer chromatography was carried out using silica gel plates (Merck 5715, 0.25 mm). Compounds were purified by flash column chromatography on silica gel 60 N (Kanto Kagaku, spherical and neutral, 40−50 μm, No. 37563-79) or by medium-pressure reversed-phase column chromatography using a Yamazen YFLC System (Yamazen Co., Osaka, Japan).

Synthesis

*2-(N-Benzyloxycarbonylamino)-4-phosphonobutanoic Acid Monosodium Salt (**6**)*. Benzyl chloroformate (51.2 g, 300 mmol) and $NaHCO_3$ (25.2 g, 300 mmol) were added portionwise over 1 h to a vigorously stirred mixture of APBA (36.6 g, 200 mmol) and NaOH (24.0 g, 600 mmol) in a mixture of H_2O (200 mL) and Et_2O (150 mL) at 0 °C. The mixture was stirred vigorously at ambient temperature for 14 h. After completion of the reaction (TLC, BuOH/AcOH/H_2O = 5:2:2, ninhydrin for the consumption of APBA), the ethereal layer was discarded. The aqueous solution was washed with Et_2O (3 × 200 mL), acidified with 6 N HCl (140 mL, 840 mmol) to pH 1, and evaporated to dryness. Acetone (500 mL) was added to the residue, and insoluble NaCl was removed by filtration. The filtrate was evaporated to give crude 2-(*N*-benzyloxycarbonylamino)-4-phosphonobutanoic acid as a colorless syrup. An aqueous solution of NaOH (7.2 g, 180 mmol, 250 mL) was added to the residue, and the resulting solution (pH 3) was evaporated to dryness. Acetone (300 mL) was added to the residue, and the mixture was stirred vigorously. The residue was crystallized spontaneously to give **6** as a colorless powder (51.8 g, yield 76%). IR (KBr) ν_{max}: 3600−2000 (br), 1722, 1531, 1454, 1415, 1340, 1247, 1173, 1117, 1051, and 919 cm^{-1}. ^{1}H NMR (300 MHz, D_2O) δ_H: 1.6−1.8 (m, 2H, PCH_2CH_2), 1.8−2.3 (m, 2H, PCH_2CH_2), 4.21 (m, 1H, α-CH), 5.13 (s, 2H, OCH_2Ph), 7.43 (m, 5H, Ph); ^{31}P NMR (121 MHz, D_2O) δ_p: 25.10. Anal. Calcd for $C_{12}H_{15}NO_7PNa\cdot0.7H_2O$: C 40.97, H 4.70, N 3.98; found: C 40.86, H 4.50, N 4.22. HRMS (FAB, glycerol) calcd for $C_{12}H_{16}NO_7PNa$ (MH + Na^+) 340.0562; found, 340.0565.

*Benzyl 2-(N-benzyloxycarbonylamino)-4-phosphonobutanoate (**7**)*. Thionyl chloride (19.5 g, 164 mmol) was added dropwise to benzyl alcohol (230 mL) at 0 °C, and the mixture was stirred for 15 min. Compound **6** (19.8 g, 58.4 mmol) was added to the solution, and the mixture was stirred at ambient temperature for 20 h. After the completion of the reaction (TLC, BuOH/AcOH/H_2O = 5:2:2, 254 nm), benzyl alcohol was removed under reduced pressure (vacuum pump, 70 °C) to give a yellow syrup. The residue was dissolved in EtOAc (300 mL), and insoluble NaCl was removed by filtration. The filtrate was washed with H_2O (3 × 50 mL) and dried over anhydrous Na_2SO_4. The solvent was evaporated, and Et_2O (300 mL) was added to the residual oil. Seed crystals were added to this partially solubilized crude product, and the mixture was stirred vigorously to give **7** as a colorless powder (21.2 g, 89%): mp 101−103 °C; IR (KBr) ν_{max}: 3600−2000 (br), 1732, 1695, 1545, 1455, 1394, 1350−850 (br), and 847 cm^{-1}. ^{1}H NMR (300 MHz, acetone-d_6) δ_H: 1.7−1.9 (m, 2H, PCH_2CH_2), 1.9−2.3(m, 2H, PCH_2CH_2), 4.38 (m, 1H, α-CH), 5.08 (s, 2H, OCH_2Ph), 5.18 (s, 2H, OCH_2Ph), 6.9 (d, J = 7.8 Hz, 1H, NH), 6.7−7.3 [br s, 2H, $P(OH)_2$], 7.2−7.5 (m, 10H, 2 × Ph); ^{31}P NMR (121 MHz, acetone-d_6) δ_p: 29.09. Anal. Calcd for $C_{19}H_{22}NO_7P$: C 56.02, H 5.44, N 3.44; found: C 56.08, H 5.38, N 3.35. HRMS (FAB, glycerol) calcd for $C_{19}H_{23}NO_7P$ (MH^+) 408.1212; found, 408.1192. Seed crystals were prepared by the filtration of a hot oversaturated solution of crude **7** in diisopropyl ether, followed by cooling at room temperature.

*Benzyl 2-(N-benzyloxycarbonylamino)-4-(dichlorophosphono)butanoate (**8**)*. Oxalyl chloride (1.41 g, 11.1 mmol) was added to a solution of **7** (2.01 g, 4.93 mmol) in dry CH_2Cl_2 (10 mL) in the presence of DMF (1 drop). Evolution of gas (CO and CO_2) was observed immediately. The mixture was stirred at 30 °C for 1 h. Volatiles were removed by vacuum evaporation followed by Ar gas flow to give the corresponding phosphonodichloridate **8** as a yellow oil. ^{1}H NMR (300 MHz, $CDCl_3$) δ_H: 2.1−2.7 (m, 4H, PCH_2CH_2), 4.53 (m, 1H, α-CH), 5.12 (s, 2H, $PhCH_2OCON$), 5.18 (d, J = 12 Hz) and 5.24 (d, J = 12 Hz) [2H, $PhCH_2O$], 5.46 (br d, 1H, J = 8.1 Hz, NH), 7.3−7.4 (m, 10H, 2 × Ph); ^{31}P NMR (121 MHz, $CDCl_3$) δ_p: 49.0. Compound **8** was used fresh for the next reaction without purification.

*General Procedure for the Synthesis of **9a**−**g**, **10**, **14a**, and **14b***. Methanol (0.16 g, 4.94 mmol) was added to a solution of **8** (4.94 mmol) in dry CH_2Cl_2 (20 mL), and the solution was cooled to −65 °C. Triethylamine (0.5 g, 4.94 mmol) was added dropwise to the solution, and the mixture was stirred at −65 °C for 30 min. The cooling bath was removed, and the mixture was allowed to stand at room temperature for an additional hour to give the crude monomethylphosphono chloridate (ca. 1:1 mixture of diastereomers) and the corresponding dimethyl phosphonate (δ_p 33.6) as the sole byproduct (ca. 25%). ^{1}H NMR (300 MHz, $CDCl_3$) δ_H: 1.7−2.4 (m, 4H, PCH_2CH_2), 3.84 (d, 3H, $^3J_{HP}$ = 13.2 Hz, CH_3OP), 4.52 (m, 1H, α-CH), 5.11 (s, 2H, $PhCH_2OCON$), 5.15−5.2 (m, 2H, $PhCH_2O$), 5.5 (br d, 1H, J = 8.1 Hz, NH), 7.3−7.4 (m, 10H, 2 × Ph); ^{31}P NMR (121 MHz, $CDCl_3$) δ_p: 44.8. The corresponding phenol (4.93 mmol) was added successively to the solution at 0 °C, and the reaction was initiated by adding Et_3N (0.50 g, 4.94 mmol). The mixture was stirred at 0 °C for 30 min and was allowed to stand at room temperature for an additional hour. After the completion of the reaction (TLC, acetone/hexane = 1:1), the reaction mixture was concentrated and diluted with EtOAc (50 mL), and the insoluble salt was removed by filtration. The filtrate was concentrated, and the crude product was purified by flash column chromatography on neutral silica gel 60 N (acetone/hexane, 1:1) to give **9a**−**g**, **10**, **14a**, and **14b** as a mixture of four stereoisomers.

*Benzyl 2-(N-benzyloxycarbonylamino)-4-[4-methoxyphenyl(methyl)phosphono]butanoate (**9a**)*. Yield, 32%, colorless oil. ^{1}H NMR (300 MHz, $CDCl_3$) δ_H: 1.8−2.3 (m, 4H, PCH_2-CH_2), 3.72 (d, $^3J_{HP}$ = 10.8 Hz, 3H, $POCH_3$), 3.77 (s, 3H, OCH_3), 4.47 (m, 1H, α-CH), 5.10 (s, 2H,OCH_2Ph), 5.17 (s, 2H, OCH_2Ph), 5.5 (br d, J = 6.9 Hz, 1H, NH), 6.81 (d, J = 9.0 Hz, 2H) and 7.1 (d, J = 7.8 Hz, 2H)(4-methoxyphenyl), 7.3 (s, 10H, 2 × Ph); ^{31}P NMR (121 MHz, $CDCl_3$) δ_p: 29.56. Anal. Calcd for $C_{27}H_{30}NO_8P$: C 61.48, H 5.73, N 2.66; found: C 61.47, H 5.82, N 2.72. HRMS (FAB, glycerol) calcd for $C_{27}H_{31}NO_8P$ (MH^+) 528.1787; found, 528.1777.

*Benzyl 2-(N-benzyloxycarbonylamino)-4-[methyl(4-methylphenyl)phosphono]butanoate (**9b**)*. Yield 40%, colorless oil. ^{1}H NMR (300 MHz, $CDCl_3$) δ_H: 1.8−2.3 (m, 4H, PCH_2-CH_2), 2.3 (s, 3H, CH_3), 3.72 (d, $^3J_{HP}$ = 11.1 Hz, 3H, $POCH_3$,), 4.46 (m, 1H, α-CH), 5.10 (s, 2H, OCH_2Ph), 5.16 (s, 2H, OCH_2Ph), 5.6 (br d, J = 6.9 Hz, 1H, NH), 7.0 (d, J = 8.4 Hz, 2H) and 7.1 (d, J = 8.4 Hz, 2H)(4-methylphenyl), 7.3 (s, 10H, 2 × Ph); ^{31}P NMR (121 MHz, $CDCl_3$) δ_p: 29.34. Anal. Calcd for $C_{27}H_{30}NO_7P$: C 63.40, H 5.91, N 2.74; found: C 63.15, H 5.91, N 2.81. HRMS (FAB, glycerol) calcd for $C_{27}H_{31}NO_7P$ (MH^+) 512.1838; found, 512.1837.

*Benzyl 2-(N-4-Nitrobenzyloxycarbonylamino)-4-[methyl-(phenyl)phosphono]butanoate (**9c**)*. Yield 48%, colorless oil. ^{1}H NMR (300 MHz, $CDCl_3$) δ_H: 1.8−2.4 (m, 4H, PCH_2-CH_2), 3.75 and 3.76 (2 × d, $^3J_{HP}$ = 11.1 Hz, 3H, $POCH_3$), 4.47 (m, 1H, α-CH), 5.20 (m, 4H, 2 × OCH_2Ph), 5.7 (2 × br d, J = 7. 8 Hz, 1H, NH), 7.1−7.4 (m, 10H, 2 × Ph), 7.5 (d, J = 7.2 Hz, 2H) and 8.2 (d, J = 7.5 Hz, 2H)(4-nitrophenyl); ^{31}P NMR (121 MHz, $CDCl_3$) δ_p: 29.25 and 29.28. Anal. Calcd for $C_{26}H_{27}N_2O_9P$: C 57.57, H 5.02, N 5.16; found: C 57.50, H 4.96, N 5.13.

*Benzyl 2-(N-benzyloxycarbonylamino)-4-[4-chlorophenyl-(methyl)phosphono]butanoate (**9d**)*. Yield 42%, colorless oil. ^{1}H NMR (300 MHz, $CDCl_3$) δ_H: 1.7−2.4 (m, 4H, PCH_2-CH_2), 3.73 (d, $^3J_{HP}$ = 11.1 Hz, 3H, $POCH_3$), 4.47 (m, 1H, α-CH), 5.10 (2 × s, 2H, OCH_2Ph), 5.17 (s, 2H, OCH_2Ph), 5.5 (br d, J = 8.4 Hz, 1H, NH), 7.09 (d, J = 8.1 Hz, 2H) and 7.26 (d, J = 8.1 Hz, 2H)(4-chlorophenyl), 7.28−7.40 (m, 10H, 2 × Ph); ^{31}P NMR (121 MHz, $CDCl_3$) δ_p: 29.69. Anal. Calcd for $C_{26}H_{27}ClNO_7P$: C 58.71, H 5.12, N 2.63; found: C 58.68, H 5.10, N 2.61. HRMS (FAB, glycerol) calcd for $C_{26}H_{28}NO_7ClP$ (MH^+) 532.1292, 534.1262; found, 532.1300, 534.1272.

*Benzyl 2-(N-benzyloxycarbonylamino)-4-[methyl(4-trifluoromethylphenyl)phosphono]butanoate (**9e**)*. Yield 54%, colorless oil. ^{1}H NMR (300 MHz, $CDCl_3$) δ_H: 1.8−2.3 (m, 4H, PCH_2CH_2), 3.75 (d, $^3J_{HP}$ = 11.1 Hz, 3H, $POCH_3$), 4.49 (m, 1H, α-CH), 5.10 (2 × s, 2H, OCH_2Ph), 5.18 (s, 2H, OCH_2Ph), 5.5 (br d, J = 6.9 Hz, 1H, NH), 7.26 (d, J = 8.4 Hz, 2H) and 7.58 (d, J = 8.4 Hz, 2H)(4-trifluoromethylphenyl), 7.3 (s, 10H, 2 × Ph); ^{31}P NMR (121 MHz, $CDCl_3$) δ_p: 29.83. Anal. Calcd for $C_{27}H_{27}F_3NO_7P$: C 57.35, H 4.81, N2.48; found: C 57.25, H 4.77, N 2.50. HRMS (FAB, glycerol) calcd for $C_{27}H_{28}F_3NO_7P$ (MH^+) 566.1556; found, 566.1546.

*Benzyl 2-(N-benzyloxycarbonylamino)-4-[4-cyanophenyl-(methyl)phosphono]butanoate (**9f**)*. Yield 38%, pale yellow oil. ^{1}H NMR (300 MHz, $CDCl_3$) δ_H: 1.8−2.4 (m, 4H, PCH_2CH_2), 3.76 (d, $^3J_{HP}$ = 11.4 Hz, 3H, $POCH_3$), 4.49 (m, 1H, α-CH), 5.10 (2 × s, 2H, OCH_2Ph), 5.18 (s, 2H, OCH_2Ph), 5.46 (br d, J = 6.6 Hz, 1H, NH), 7.3 (d, J = 7.5 Hz, 2H) and 7.60 (dd, J = 1.6 and 8.4 Hz)(4-cyanophenyl), 7.4 (s, 10H, 2 × Ph); ^{31}P NMR (121 MHz, $CDCl_3$) δ_p: 30.05. Anal. Calcd for $C_{27}H_{27}N_2O_7P$: C 62.07, H 5.21, N 5.36; found: C 61.93, H 5.15, N 5.47.

*Benzyl 2-(N-benzyloxycarbonylamino)-4-[methyl(4-nitrophenyl)phosphono]butanoate (**9** g)*. Yield 45%, pale yellow oil. ^{1}H NMR (300 MHz, $CDCl_3$) δ_H: 1.8−2.3 (m, 4H, PCH_2-CH_2), 3.77 (d, $^3J_{HP}$ = 11.1 Hz, 3H, $POCH_3$), 4.5 (m, 1H, α-CH), 5.10 (m, 2H) and 5.18 (m, 2H)(2 × OCH_2Ph), 5.5 (br d, J = 6.9 Hz, 1H, NH), 7.31 (d, J = 9.3 Hz, 2H) and 8.20 (d, J = 9.0 Hz, 2H)(4-nitrophenyl), 7.3 (s, 10H, 2 × Ph); ^{31}P NMR (121 MHz, $CDCl_3$) δ_p: 30.20. Anal. Calcd for $C_{26}H_{27}N_2O_9P$: C 57.57, H 5.02, N 5.16; found: C 57.35, H 5.11, N 5.17; HRMS (FAB, glycerol) calcd for $C_{26}H_{28}N_2O_9P$ (MH^+) 543.1532; found, 543.1537.

*Benzyl 2-(N-benzyloxycarbonylamino)-4-[methyl(4-methylumbelliferyl)phosphono]butanoate (**10**)*. Yield 40%, colorless oil. ^{1}H NMR (300 MHz, $CDCl_3$) δ_H: 1.8−2.3 (m, 4H, PCH_2-CH_2), 2.42 (s, 3H, 4′−CH_3), 3.77 (d, $^3J_{HP}$ = 11.1 Hz, 3H, $POCH_3$), 4.49 (m, 1H, α-CH), 5.11 (s, 2H, OCH_2Ph), 5.19 (s, 2H, OCH_2Ph), 5.5 (br d, J = 6.9 Hz, 1H, NH), 6.25 (s, 1H, 3′-H), 7.14 (s, 1H, 8′-H), 7.16 (d, 1H, J = 9.0 Hz, 5′-H), 7.3−7.4 (s, 10H, 2 × Ph), 7.53 (d, 1H, J = 8.4 Hz, 6′-H); ^{31}P NMR (121 MHz, $CDCl_3$) δ_p: 30.07. Anal. Calcd for $C_{30}H_{30}NO_9P$: C 62.18, H 5.22, N 2.42; found C 62.09, H 5.25, N 2.54. HRMS (FAB, glycerol) calcd. for $C_{30}H_{31}NO_9P$ (MH^+) 580.1737; found, 580.1727.

*N-(2-Hydroxybutanoyl)glycine benzyl ester (**11**)*. A mixture of lithium 2-hydroxybutyrate (racemic, 1.50 g, 13.6 mmol), glycine benzyl ester *p*-toluenesulfonate salt (4.60 g, 13.6 mmol) and 1-hydroxybenzotriazole hydrate (HOBt) (1.84 g, 13.6 mmol) in acetonitrile (80 mL) was stirred at room temperature for 20 min to give a fine suspension. To this mixture, was added 1-(3-dimethylaminopropyl)-3-ethylcarbodiimide hydrochloride (EDC) (2.61 g, 13.6 mmol), and the mixture was stirred at room temperature overnight. The reaction mixture was filtered, and the filtrate was evaporated. The residual oil was dissolved in EtOAc (200 mL), washed successively with 1 N HCl, sat. $NaHCO_3$ and sat. NaCl, and dried over anhydrous Na_2SO_4. The solvent was evaporated, and the crude product was purified by flash column chromatography on silica gel (Merck, No. 9385) (hexane/EtOAc = 1:2) to give *N*-(2-hydroxybutanoyl)glycine benzyl ester as a colorless syrup (1.67 g, 49%). ^{1}H NMR (300 MHz, $CDCl_3$) δ_H: 0.99 (t, J = 7.5 Hz, 3H, CH_3CH_2), 1.70 (ddq, J = 7.2, 7.2 and 15 Hz, 1H) and 1.89 (ddt, J = 4.2, 7.2 and 15 Hz, 1H) (CH_3CH_2), 4.08 (dd, J = 5.6 and 18 Hz, 1H, $NHCH_2CO$), 4.14 (dd, J = 3.9 and 7.5 Hz, 1H, CH), 4.16 (dd, J = 5.7 and 18 Hz, 1H, $NHCH_2CO$), 7.10 (br t, 1H, NH), 7.3−7.4 (s, 5H, Ph). HRMS (FAB, glycerol) calcd. for $C_{13}H_{18}NO_4$ (MH^+) 252.1236; found, 252.1232.

*Benzyl 2-(N-benzyloxycarbonylamino)-4-{1-[N-(benzyloxycarbonylmethyl)carbamoyl] propyl(phenyl)phosphono}butanoate (**12**)*. Compound **12** was synthesized from **8** by stepwise reaction with phenol and alcohol **11** by the same procedure described for the synthesis of **9a**−**g**. Yield 15% (a mixture four diastereomers), colorless oil. IR (KBr) ν_{max}: 3600−3100 (br), 3064, 3033, 2972, 2941, 1747, 1685, 1591, 1533, 1491, 1455, 1387, 1346, 1255, 1201, 1051, 1002, 937, and 740 cm^{-1}. ^{1}H NMR (300 MHz, $CDCl_3$) δ_H: 0.81 and 0.92 (2 × t, J = 7.5 Hz, 3H, CH_2CH_3), 1.7−2.4 (m, 6H, PCH_2CH_2 and CH_2CH_3), 3.7−4.1 (m, 2H, $NHCH_2CO$), 4.5 (m, 1H,

α-CH), 4.9 (m, H, POC*H*CO), 5.1−5.2 (m, 6H, 3 × PhCH_2O), 5.5 (br m, 1H, NH), 5.6 and 5.8 (2 × br m, 1H, NH), 7.1−7.4 (m, 20H, 4 × Ph); ^{31}P NMR (121 MHz, $CDCl_3$) δ_p: 28.05 (24%), 28.31 (17%), 28.47 (25%), 28.66 (34%). Anal. Calcd for $C_{38}H_{41}N_2O_{10}P$: C 63.68, H 5.77, N 3.91; found C 63.66, H 5.85, N 3.86. HRMS (FAB, glycerol) calcd for $C_{38}H_{42}N_2O_{10}P$ (MH^+) 717.2577; found, 717.2578.

*Benzyl 3-hydroxyphenylacetate (**13a**)* and *Benzyl 4-hydroxyphenylacetate (**13b**)*. Phenols **13a** and **13b** were prepared by benzylation (BnBr, K_2CO_3, acetonitrile) of the corresponding acid according to the reported procedure (*44*).

*Benzyl 2-(N-benzyloxycarbonylamino)-4-{[3-(benzyloxycarbonylmethyl)phenyl](methyl)phosphono}butanoate (**14a**).* Yield 31%, colorless oil. IR (KBr) ν_{max}: 3600−2300 (br), 1736, 1608, 1587, 1533, 1448, 1379, 1340, 1250, 1174, 1047, and 980 cm^{-1}. ^{1}H NMR (300 MHz, $CDCl_3$) δ_H: 1.8−2.4 (m, 4H, PCH_2CH_2), 3.64 (s, 2H, CH_2COOBn), 3.71 (d, $^3J_{HP}$ = 10.8 Hz, 3H, $POCH_3$), 4.5 (m, 1H, α-CH), 5.10 and 5.12 (2 × s, 4H, 2 × OCH_2Ph), 5.17 (s, 2H, CHCOOCH_2Ph), 5.6 (br m, 1H, NH), 7.06−7.11 (m) and 7.22 (m) (4H, POC_6H_4), 7.3−7.5 (m, 15H, 3 × Ph); ^{31}P NMR (121 MHz, $CDCl_3$) δ_p: 29.31. Anal. Calcd for $C_{35}H_{36}NO_9P$: C 65.11, H 5.62, N 2.17; found: C 65.36, H 5.38, N 2.11. HRMS (FAB, glycerol) calcd for $C_{35}H_{37}NO_9P$ (MH^+) 646.2206; found, 646.2233.

*Benzyl 2-(N-benzyloxycarbonylamino)-4-{[4-(benzyloxycarbonylmethyl)phenyl](methyl)phosphono}butanoate (**14b**).* Yield 40%, colorless oil. IR (KBr) ν_{max}: 3600−2000 (br), 1731, 1508, 1455, 1340, 1259, 1217, 1153, 1047, and 919 cm^{-1}. ^{1}H NMR (300 MHz, $CDCl_3$) δ_H: 1.8−2.4 (m, 4H, PCH_2CH_2), 3.62 (s, 2H, CH_2COOBn), 3.73 (d, $^3J_{HP}$ = 11.1 Hz, 3H, $POCH_3$), 4.5 (m, 1H, α-CH), 5.10 and 5.12 (2 × s, 4H, 2 × OCH_2Ph), 5.17 (s, 2H, CHCOOCH_2Ph), 5.5 (br m, 1H, NH), 7.10 (d, J = 7.8 Hz) and 7.22 (d, J = 8.4 Hz) (4H, POC_6H_4), 7.3−7.4 (m, 15H, 3 × Ph); ^{31}P NMR (121 MHz, $CDCl_3$) δ_p: 29.36. Anal. Calcd for $C_{35}H_{36}NO_9P$: C 65.11, H 5.62, N 2.17; found: C 65.01, H 5.71, N 2.25. HRMS (FAB, glycerol) calcd for $C_{35}H_{37}NO_9P$ (MH^+) 646.2206; found, 646.2605.

*General Procedure for the Synthesis of **2a**−**g**, **3**, **4**, **5a**, and **5b***

Method A. Compound **9a**−**c**, **12**, **14a**, or **14b** (1.37 mmol) was dissolved in MeOH/H_2O (2:1, 30 mL) or in AcOH (30 mL). Hydrogen gas was passed through the solution in the presence of 5% Pd-C (270 mg) for 2 h at ambient temperature. Pd-C was removed by filtration through Celite, and the filtrate was evaporated. In most cases, the products were pure enough without purification and were lyophilized from water to give the final product **2a**−**c**, **4**, **5a**, and **5b** as a colorless and slightly hygroscopic solid. If necessary, the product was purified by medium-pressure reversed-phase column chromatography on an ODS-S-50B (Yamazen Co., Osaka, Japan). The column was eluted (6 mL/min) with a linear gradient of 30−60% MeOH/H_2O, and the fractions containing the product (TLC, BuOH/AcOH/H_2O, 5:2:2, ninhydrin) were collected and lyophilized.

Method B. Aluminum chloride (0.55 g, 4.11 mmol) was added to a solution of **9d**−**g** or **10** (1.37 mmol) and anisole (0.89 g, 8.22 mmol) in dry nitromethane (10 mL). The solution was stirred at room temperature for 1 h, and H_2O (20 mL) was added. After 10 min, the reaction mixture was washed with Et_2O (3 × 50 mL) to remove nitromethane. The aqueous layer was diluted with MeOH (final concn of ca. 30%) and was passed through a short column (ca. 8 cm) of neutral silica gel 60 N to remove $Al(OH)_3$. The eluate (ca. 30 mL) was applied directly to medium-pressure reversed-phase column chromatography on an ODS-S-50B. The column was eluted (6 mL/min) with a linear gradient of 30−60% MeOH/H_2O, and the fractions containing the product (TLC, BuOH/AcOH/H_2O, 5:2:2, ninhydrin) were collected and lyophilized to afford **2d**−**g** and **3** as colorless solids.

*2-Amino-4-[(4-methoxyphenyl)(methyl)phosphono]-butanoic Acid (**2a**).* Yield 58%, colorless solid. IR (KBr) ν_{max}: 3600−2300 (br), 1635, 1597, 1508, 1456, 1409, 1363, 1252, 1207, 1029, 953, and 840 cm^{-1}. ^{1}H NMR (300 MHz, D_2O) δ_H: 2.1−2.3 (m, 4H, PCH_2CH_2), 3.8−3.9 (m, 7H, α-CH, POCH_3 and PhOCH_3), 7.03 (d, J = 9.3 Hz, 2H) and 7.20 (d, J = 8.4 Hz, 2H)(4-methoxyphenyl); ^{31}P NMR (121 MHz, D_2O) δ_p: 32.88; Anal. Calcd for $C_{12}H_{18}NO_6P\cdot 0.5H_2O$: C 46.16, H 6.13, N 4.49; found: C 46.15, H 6.20, N 4.45. HRMS (FAB, glycerol) calcd for $C_{12}H_{19}NO_6P$ (MH^+) 304.0950; found, 304.0945.

*2-Amino-4-[methyl(4-methylphenyl)phosphono]butanoic Acid (**2b**).* Yield 51%, colorless solid. IR (KBr) ν_{max}: 3600−2300 (br), 1623, 1540, 1508, 1448, 1409, 1365, 1205, 1047, 941, and 833 cm^{-1}. ^{1}H NMR (300 MHz, D_2O) δ_H: 2.1−2.3 (m, 4H, PCH_2CH_2), 2.31 (s, 3H, PhCH_3), 3.81 (m, 1H, α-CH), 3.85 (d, $^3J_{HP}$= 12.3 Hz, 3H, $POCH_3$), 7.11 (d, J = 8.1 Hz, 2H) and 7.27 (d, J = 7.8 Hz, 2H)(4-methylphenyl); ^{31}P NMR (121 MHz, D_2O) δ_p: 32.53. Anal. Calcd for $C_{12}H_{18}NO_5P\cdot 0.3H_2O$: C 49.25, H 6.41, N 4.79; found: C 49.28, H 6.32, N 4.77. HRMS (FAB, glycerol) calcd for $C_{12}H_{19}NO_5P$ (MH^+) 288.2567; found, 288.1009.

*2-Amino 4-[methyl(phenyl)phosphono]butanoic Acid (**2c**).* Yield 48%, colorless solid. IR (KBr) ν_{max}: 3600−2300 (br), 1634, 1593, 1491, 1455, 1403, 1345, 1208, 1045, 936, and 832 cm^{-1}. ^{1}H NMR (300 MHz, D_2O) δ_H: 2.1−2.4 (m, 4H, PCH_2CH_2), 3.88 (d, $^3J_{HP}$= 11.1 Hz, 3H, $POCH_3$), 3.85 (m, 1H, α-CH), 7.25 (d, J = 7.8 Hz, 2H), 7.33 (t, J = 7.2 Hz, 1H) and 7.48 (t, J = 7.8 Hz, 2H)(phenyl); ^{31}P NMR (121 MHz, D_2O) δ_p: 32.55. Anal. Calcd for $C_{11}H_{16}NO_5P\cdot 0.6H_2O$: C 46.32, H 6.10, N 4.93; found: C 46.36, H5.97, N 5.06. HRMS (FAB, glycerol) calcd for $C_{11}H_{17}NO_5P$ (MH^+) 274.0844; found, 274.0840.

*2-Amino 4-[4-chlorophenyl(methyl)phosphono]butanoic Acid (**2d**).* Yield 57%, colorless solid. IR (KBr) ν_{max}: 3600−2300 (br), 1623, 1595, 1488, 1405, 1358, 1213, 1093, 1045, 928, and 835 cm^{-1}. ^{1}H NMR (300 MHz, D_2O) δ_H: 2.1−2.3 (m, 4H, PCH_2CH_2), 3.83 (m, 1H, α-CH), 3.86 (d, $^3J_{HP}$= 11.4 Hz, 3H, $POCH_3$), 7.21 (d, J = 7.8 Hz, 2H) and 7.46 (d, J = 8.7 Hz, 2H)(4-chlorophenyl); ^{31}P NMR (121 MHz, D_2O) δ_p: 32.69. Anal. Calcd for $C_{11}H_{15}ClNO_5P\cdot 0.4H_2O$: C 41.96, H 5.06, N 4.45; found: C 42.17, H 5.03, N 4.53. HRMS (FAB, glycerol) calcd for $C_{11}H_{16}ClNO_5P$ (MH^+) 308.0455; found, 308.0466.

*2-Amino-4-[methyl(4-trifluoromethylphenyl)phosphono]-butanoic Acid (**2e**).* Yield 63%, colorless solid. IR (KBr) ν_{max}: 3600−2300 (br), 1646, 1616, 1516, 1403, 1338, 1225, 1174, 1121, 1070, 1047, 933, and 850 cm^{-1}. ^{1}H NMR (300 MHz, D_2O) δ_H: 2.1−2.4 (m, 4H, PCH_2CH_2), 3.85 (m, 1H, α-CH), 3.89 (2 × d, $^3J_{HP}$= 11.4 Hz, 3H, $POCH_3$), 7.41 (d,

J = 8.4 Hz, 2H) and 7.80 (d, J = 8.7 Hz, 2H)(4-trifluoromethylphenyl); ^{31}P NMR (121 MHz, D_2O) δ_p: 32.58. Anal. Calcd for $C_{12}H_{15}F_3NO_5P\cdot0.8H_2O$: C 40.53, H 4.70, N 3.94; found: C 40.63, H 4.41, N 4.20. HRMS (FAB, glycerol) calcd for $C_{12}H_{16}F_3NO_5P$ (MH^+) 342.0178; found, 342.0709.

*2-Amino-4-[4-cyanophenyl(methyl)phosphono]butanoic Acid (**2f**).* Yield 70%, colorless solid. IR (KBr) ν_{max}: 3600−2300 (br), 2231, 1647, 1604, 1500, 1412, 1360, 1225, 1176, 1105, 1045, 926, and 837 cm^{-1}. ^{1}H NMR (300 MHz, D_2O) δ_H: 2.1−2.4 (m, 4H, PCH_2CH_2), 3.82 (m, 1H, α-CH), 3.88 (d, $^3J_{HP}$= 11.4 Hz, 3H, $POCH_3$), 7.39 (d, J = 8.7 Hz, 2H) and 7.83 (d, J = 8.1 Hz, 2H)(4-cyanophenyl); ^{31}P NMR (121 MHz, D_2O) δ_p: 32.61. Anal. Calcd for $C_{12}H_{15}N_2O_5P\cdot0.3H_2O$: C 47.47, H 5.18, N 9.23; found: C 47.56, H 5.09, N 9.24. HRMS (FAB, glycerol) calcd for $C_{12}H_{16}N_2O_5P$ (MH^+) 299.0797; found, 299.0789.

*2-Amino-4-[methyl(4-nitrophenyl)phosphono]butanoic Acid (**2g**).* Yield 70%, colorless solid. IR (KBr) ν_{max}: 3600−2300 (br), 2231, 1629, 1590, 1490, 1411, 1342, 1292, 1223, 1164, 1108, 1045, 931, and 860 cm^{-1}. ^{1}H NMR (300 MHz, D_2O) δ_H: 2.1−2.4 (m, 4H, PCH_2CH_2), 3.88 (m, 1H, α-CH), 3.91 (d, $^3J_{HP}$= 11.4 Hz, 3H, $POCH_3$), 7.44 (d, J = 8.7 Hz, 2H) and 8.33 (d, J = 9.0 Hz, 2H)(4-nitrophenyl); ^{31}P NMR (121 MHz, D_2O) δ_p: 32.63. Anal. Calcd for $C_{11}H_{15}N_2O_7P\cdot1.5H_2O$: C 38.27, H 5.26, N 8.11; found: C 38.25, H 5.05, N 8.20. HRMS (FAB, glycerol) calcd for $C_{11}H_{16}N_2O_7P$ (MH^+) 319.0695; found, 319.0703.

*2-Amino-4-[methyl(4-methylumbelliferyl)phosphono]butanoic Acid (**3**).* Yield 49%, colorless solid. IR (KBr) ν_{max}: 3600−2300 (br), 1733, 1716, 1612, 1506, 1446, 1390, 1270, 1230, 1137, 1070, 1043, 989, 920, and 833 cm^{-1}. ^{1}H NMR (300 MHz, D_2O) δ_H: 2.1−2.4 (m, 4H, PCH_2CH_2), 2.49 (s, 3H, 4′-CH_3), 3.86 (m, 1H, α-CH), 3.91 (2 × d, $^3J_{HP}$= 11.4 Hz, 3H, $POCH_3$), 6.4 (s, 1H, 3′-H), 7.27 (d, J = 8.1 Hz, 1H, 5′-H), 7.28 (s, 1H, 8′-H), 7.84 (d, J = 8.1 Hz, 1H, 6′-H); ^{31}P NMR (121 MHz, D_2O) δ_p: 32.69. Anal. Calcd for $C_{15}H_{18}NO_7P\cdot0.3H_2O$: C 49.95, H 5.20, N 3.88; found: C 49.86, H 5.14, N 3.84. HRMS (FAB, glycerol) calcd for $C_{15}H_{19}NO_7P$ (MH^+) 356.0899; found, 356.0904.

*2-Amino-4-{1-[N-(carboxymethyl)carbamoyl]propyl(phenyl)phosphono}butanoic Acid (**4**).* Yield 18% (a mixture of four diastereomers), colorless solid. IR (KBr) ν_{max}: 3600−2300 (br), 1668, 1652, 1593, 1541, 1489, 1455, 1398, 1348, 1205, 1051, 1007, 941, and 769 cm^{-1}. ^{1}H NMR (300 MHz, D_2O) δ_H: 0.84 (t, 3H, J = 7.5 Hz, CH_2CH_3), 1.6−1.9 (m, 3H) and 2.2−2.4 (m, 3H) (PCH_2CH_2 and CH_2CH_3), 3.8−4.0 (m, 3H, α-CH and $NHCH_2COOH$), 4.9 (m, H, POCHCO), 7.26 (d, J = 8.1 Hz, 2H), 7.33 (t, J = 7.3 Hz, 1H) and 7.46 (t, J = 7.8 Hz, 2H)(phenyl); ^{31}P NMR (121 MHz, D_2O) δ_p: 30.91. HRMS (FAB, glycerol) calcd for $C_{16}H_{24}N_2O_8P$ (MH^+) 403.1270; found, 403.1275.

*2-Amino-4-{[3-(carboxymethyl)phenyl](methyl)phosphono}butanoic Acid (**5a**).* Yield 51%, colorless solid. IR (KBr) ν_{max}: 3600−2300 (br), 1718, 1637, 1587, 1489, 1446, 1406, 1346, 1236, 1149, 1045, 984, 939, 885 and 860 cm^{-1}. ^{1}H NMR (300 MHz, D_2O) δ_H: 2.2−2.3 (m, 4H, PCH_2CH_2), 3.68 (s, 2H, $PhCH_2COOH$), 3.8−3.9 (m, 1H, α-CH), 3.86 (d, $^3J_{HP}$= 11.1 Hz) and 3.87 (d, $^3J_{HP}$= 11.1 Hz) (3H, $POCH_3$), 7.15 (s, 2H), 7.20 (d, J= 7.8 Hz, 1H) and 7.41 (m, 1H) (phenyl); ^{31}P NMR (121 MHz, D_2O) δ_p: 32.52. Anal. Calcd for $C_{13}H_{18}NO_7P\cdot0.6H_2O$: C 45.65, H 5.66, N 4.09; found: C 45.56, H 5.43, N 4.04. HRMS (FAB, glycerol) calcd for $C_{13}H_{19}NO_7P$ (MH^+) 332.0899; found, 332.0894.

*2-Amino-4-{[4-(carboxymethyl)phenyl](methyl)phosphono}butanoic Acid (**5b**).* Yield 64%, colorless solid. IR (KBr) ν_{max}: 3600−2300 (br), 1718, 1630, 1508, 1448, 1406, 1346, 1215, 1169, 1045, 939, and 825 cm^{-1}. ^{1}H NMR (300 MHz, D_2O) δ_H: 2.2−2.3 (m, 4H, PCH_2CH_2), 3.67 (s, 2H, $PhCH_2COOH$), 3.8−4.0 (m, 1H, α-CH), 3.88 (d, $^3J_{HP}$= 11.4 Hz, 3H, $POCH_3$), 7.21 (d, J = 8.1 Hz, 2H) and 7.35 (d, J = 8.4 Hz, 2H)(phenyl); ^{31}P NMR (121 MHz, D_2O) δ_p: 32.56. Anal. Calcd for $C_{13}H_{18}NO_7P\cdot1.0\ H_2O$: C 44.70, H 5.77, N 4.01; found: C 44.42, H 5.43, N 3.83. HRMS (FAB, glycerol) calcd for $C_{13}H_{19}NO_7P$ (MH^+) 332.0899; found, 332.0900.

Hydrolytic Stability of Inhibitors. The hydrolysis of the inhibitors **2a**−**g**, **3**, **4**, **5a**, and **5b** was monitored with ^{31}P NMR (121 MHz) by incubating the compounds in D_2O at 23 °C. The stability of **2g** was also investigated in D_2O at 23 °C under varying pH conditions: 1 M Na_2CO_3, 1 M $NaHCO_3$, 1 M CH_3COOD, 1 M CF_3COOD, and 1 M DCl. The ratio of the remaining phosphonate diesters and the hydrolyzed product, 2-amino-4-[hydrogen(methyl)phosphono]butanoic acid (δ_p: = 27.2), was calculated from the integration of the ^{31}P NMR peak areas.

Enzyme Assay. The hydrolytic activity of *E. coli* GGT was fluorimetrically measured by following the release of 7-amino-4-methylcoumarin (AMC) using 0.2 μM 7-(*N*-γ-glutamylamino)-4-methylcoumarin (γ-Glu-AMC) as the substrate at 25 °C (pH 5.5) (*46*). Assays were initiated by adding 10 μL of enzyme stock solution to 100 mM succinate−NaOH buffer (pH 5.5) in a total volume of 1 mL containing 100 μL of γ-Glu-AMC stock solution (2 μM in water) at 25 °C (a final γ-Glu-AMC concentration of 0.2 μM). The release of AMC was monitored continuously for 10 min with a Hitachi F-2000 spectrophotometer (350 nm excitation, 440 nm emission). AMC concentrations were calculated using a standard calibration curve of fluorescence intensity (F) versus AMC concentration (C): $\Delta F/\Delta C$ = 0.11 nM^{-1}. The fluorescence intensity was proportional to the concentration of AMC up to 2.0 μM. The Michaelis constant (K_m) for γ-Glu-AMC was determined to be 0.2 μM under these conditions. The hydrolytic activity of human GGT was measured under the same conditions, except that the final substrate concentration was 4.0 μM in 100 mM succinate−NaOH buffer. The K_m value for γ-Glu-AMC was determined to be 12.6 μM under these conditions.

Time-Dependent Inhibition Assay. The inhibition of GGT was measured using a continuous or discontinuous assay method under pseudo-first-order rate conditions. For the continuous assay, a typical run was as follows: enzyme was added to a preincubated mixture of varying concentrations of the inhibitor and the substrate (final concentrations of 0.2 and 4.0 μM γ-Glu-AMC for *E. coli* and human GGT, respectively) in 100 mM sodium succinate buffer (pH 5.5) at 25 °C. Time-dependent inhibition of the enzyme was followed by continuously monitoring the release of AMC for 10 min. The resulting progress curves were analyzed by fitting the data to the first-order rate eq 1 to calculate the observed pseudo-first-order rate constants for enzyme inactivation (k_{obs}) using the KaleidaGraph v.3.5 program package (Synergy Software).

$$[P] = [P]_\infty[1 - \exp(-k_{obs}\, t)] \quad (1)$$

where [P] and $[P]_\infty$ are the concentrations of AMC formed at time t and at time approaching infinity, respectively. Because the replot of k_{obs} versus inhibitor concentration ([I]) exhibited no saturation under standard inhibitor concentrations, the second-order rate constant for enzyme inactivation (k_{on}) was calculated according to eq 2 derived from the kinetic mechanism described below

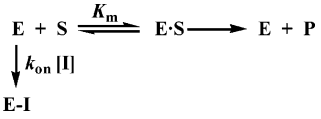

$$k_{obs} = k_{on}[I]/(1 + [S]/K_m) \quad (2)$$

where S is the substrate γ-Glu-AMC; [S] and K_m are 0.2 and 0.2 μM (*E. coli* GGT), and 4.0 and 12.6 μM (human GGT). For **5a** and **5b**, the plot of k_{obs} versus [I] reached saturation at higher inhibitor concentrations (180 μM and 9.0 mM, respectively), and the values of the dissociation constant (K_i) and the first-order rate constant for enzyme inactivation (k_{inact}) were calculated according to eq 3 (*47*) derived from the following kinetic mechanism.

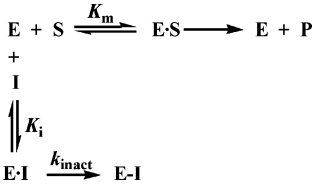

$$k_{obs} = k_{inact}[I]/\{K_i(1 + [S]/K_m) + [I]\} \quad (3)$$

For the discontinuous assay (for human GGT with **2a** and **2b**), the enzyme (final concn of 0.5 μg/mL of enzyme) was incubated in the presence of varying concentrations of the inhibitor at 25 °C in 100 mM succinate−NaOH (pH 5.5). An aliquot (10 μL) was taken at various time intervals and was assayed for residual activity. The values of k_{obs} were obtained by fitting the residual activities to the eq 4

$$a_t/a_0 = \exp(-k_{obs}\, t) \quad (4)$$

where a_t is the residual activity at time t, and a_0 is the initial activity before inactivation ($t = 0$). Nonlinear regression analyses of kinetic data were also performed using the KaleidaGraph program. The values for k_{on} were calculated according to eq 5.

$$k_{on} = k_{obs}/[I] \quad (5)$$

RESULTS AND DISCUSSION

Synthesis and Stability of Phosphonate Diesters. The phosphonate diesters **2a**−**g**, **3**, **4**, **5a**, and **5b** were synthesized as shown in Scheme 2. The amino group of racemic 2-amino-4-phosphonobutanoic acid (APBA) (*42*, *43*) was protected by the benzyloxycarbonyl (Z) group. The protected phosphonic acid (Z-APBA) was obtained previously as a syrup, and its purification required reversed-phase column chromatography (*39*). We found, however, that the corresponding monosodium salt was crystallized readily from acetone to give pure product **6** as a colorless and non-hygroscopic

Scheme 2: Synthesis of Phosphonate Diesters **2a**−**g**, **3**, **4**, **5a**, and **5b**

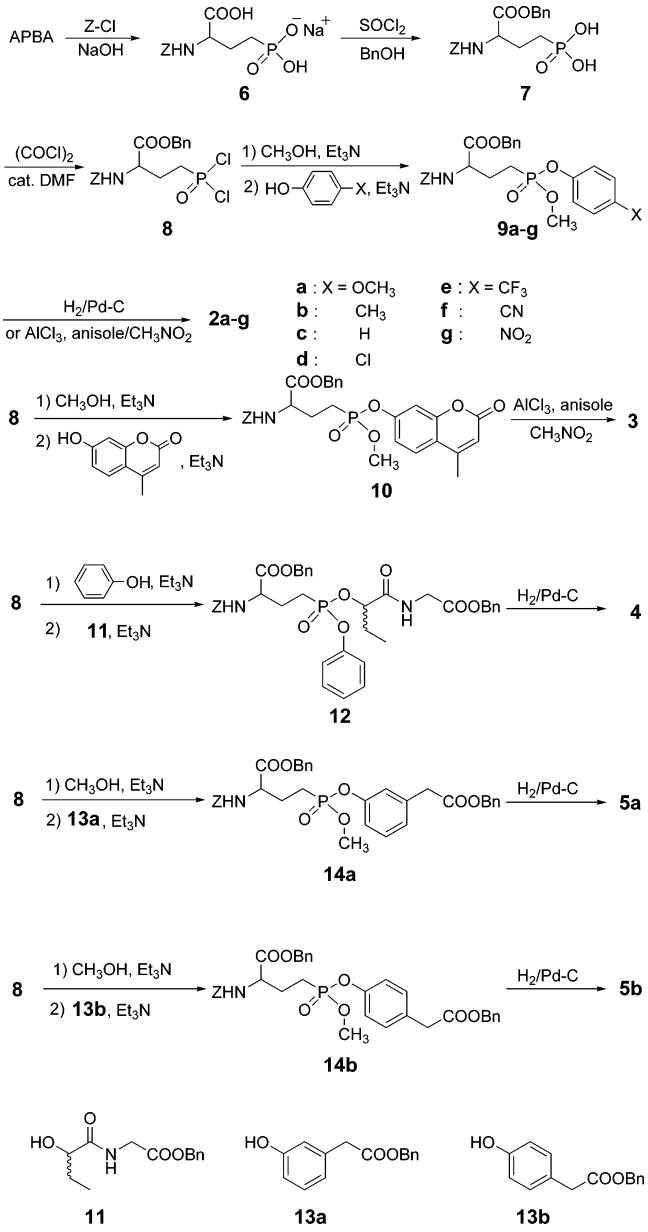

powder, thereby greatly improving the purification procedure so that it is amenable to a large scale synthesis. α-Carboxy group **6** was protected by selective esterification under acidic conditions to afford benzyl ester **7** with a free γ-phosphono group. Compound **7** was also obtained in high yield as non-hygroscopic crystals. Phosphonic acid **7** was converted to the phosphonic dichloride **8**, a common intermediate for the synthesis of a series of the phosphonate diesters by stepwise esterification. Thus, dichloride **8** was allowed to react with one equivalent of methanol with Et_3N as a catalyst (*48*) to afford the monomethyl phosphonochloridate as a major product, but the corresponding dimethyl phosphonate was also formed (ca. 25%). Because the phosphonyltriethylammonium intermediate (*48*) was so reactive, Et_3N was added carefully at low temperatures (ca. −65 °C) after the addition of methanol to minimize the formation of the dimethyl phosphonate. The crude monomethyl phosphonochloridate was treated with phenols and Et_3N to give the

corresponding phosphonate diesters **9a**−**g**, **10**, **14a**, and **14b**. Phosphonate **12** was obtained by successively treating dichloride **8** with phenol and alcohol **11**.

The benzyl protecting groups of **9a**−**c**, **12**, **14a**, and **14b** were removed by conventional hydrogenolysis with Pd-C as a catalyst (Method A), whereas those in phosphonates **9d**−**g** and **10** containing the chloro-, trifluoromethyl-, cyano-, and nitrophenyl groups and the 4-methylumbelliferyl group were removed by a Lewis-acid promoted deprotection method using $AlCl_3$ and anisole (Method B; see Experimental Procedures) (*49*) to avoid the reduction of these functional groups. The latter method worked well for cleaving the benzyl protecting groups but was problematic in product isolation: the remaining $Al(OH)_3$ promoted the cleavage of the methyl phosphonate to give the corresponding monophenyl phosphonates. Interestingly, the methyl phosphonate was neither cleaved under the $AlCl_3$−anisole reaction conditions nor hydrolyzed in a diluted aqueous solution containing $Al(OH)_3$ after aqueous workup but was selectively hydrolyzed to give the corresponding monophenyl phosphonate when the aqueous solution was concentrated. This was attributed to the coordination of Lewis acidic $Al(OH)_3$ to the phosphoryl oxygen when most of the Lewis basic water was removed. The coordination of Al^{3+} probably catalyzed the S_N2 type C−O bond fission of the methyl phosphonate by the nucleophilic attack of water on the methyl carbon. This mechanism was supported by the fact that no hydrolysis was observed with the otherwise hydrolytically more labile phenyl ester bond of the phosphonates. In order to avoid demethylation, $Al(OH)_3$ was removed by passing the product mixture through a neutral silica gel column before concentration of the product, followed by purification with reversed-phase column chromatography.

The phosphonate diesters **2a**−**g**, **3**, **4**, **5a**, and **5b** were obtained as a mixture of four or eight stereoisomers with respect to the chiral α-carbon, the phosphorus and the chiral 2-hydroxybutyryl carbon atom (for compound **4**). Although no attempts were successful in separating the diastereomers or directly determining the diastereomeric ratio by spectroscopic methods, each phosphonate was expected to be a 1:1 mixture of the diastereomers with respect to the chiral phosphorus because 2-amino-4-[methyl(3-nitrophenyl)phosphono]-butanoic acid synthesized by the same procedure consisted of an equal amount of two diastereomers (^{31}P NMR; see Supporting Information).

The hydrolytic stability of **2a**−**g** and **3** was examined in D_2O at 23 °C. Phenyl phosphonates **2a**−**e** with electron-donating groups or weak electron-withdrawing groups were very stable, and no hydrolysis was observed in 12 h. In contrast, phosphonates **3**, **2f**, and **2g** with good leaving groups were hydrolyzed by 6, 12, and 49%, respectively, to give the monomethyl phosphonate under the same conditions. As expected, the rate of hydrolysis was increased by increasing the leaving group ability of the phenols. Compound **2g**, the least stable phosphonate, was subjected to further investigation for stability under varying pH conditions at 23 °C. Phosphonate **2g** was hydrolyzed completely in 1 M Na_2CO_3 or $NaHCO_3$ in 12 h, but the hydrolysis was reduced to ca. 40% in 1 M CH_3COOD. Under highly acidic conditions (1 M CF_3COOD or DCl), compound **2g** was quite stable, and no hydrolysis was observed in 24 h. These results indicated that the hydrolysis of the phosphonate diesters was base-catalyzed and was consistent with the hydrolysis of neutral phosphate triesters, in which hydrolysis proceeds with a tight and associative transition state (*50*).

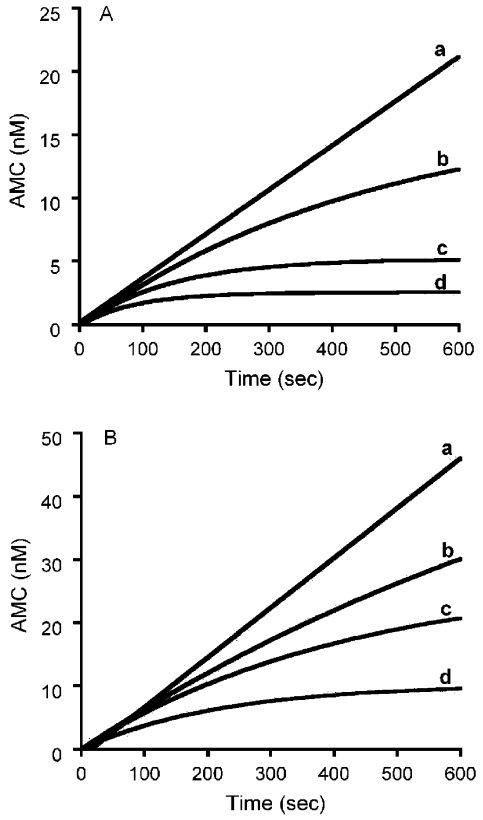

FIGURE 2: Typical time-dependent inhibition of GGT by phosphonate diesters. (A) Progress curves of *E. coli* GGT with 0.2 μM γ-Glu-AMC as the substrate at pH 5.5 in the presence of varying concentrations of **2d**: (a) 0, (b) 7.1, (c) 21, and (d) 36 μM. (B) Progress curves of human GGT with 4.0 μM γ-Glu-AMC at pH 5.5 in the presence of varying concentrations of **2d**: (a) 0, (b) 0.36, (c) 0.72, and (d) 1.4 mM.

*Inactivation of E. coli and Human GGT by **2a**−**g** and **3**.* Phosphonate diesters **2a**−**g** and **3** were found to serve as highly potent and time-dependent inhibitors of both *E. coli* and human GGTs. Figure 2 shows a typical time-dependent inhibition profile observed with **2d**. Enzyme activity was decreased as a function of time and the concentration of the inhibitor. In each case, the enzyme was totally inactivated in the end, and no activity was recovered after a prolonged dialysis of the inactivated enzyme (Supporting Information). These results were consistent with the proposed inhibition mechanism (Figure 1), where the phosphonate diesters **2a**−**g** and **3** reacted covalently with the catalytic Thr residue of GGT in a mechanism-based manner to form a phosphonylated enzyme, as was confirmed with the corresponding monofluorophosphono derivative (*39*).

The time-dependent inhibition curves of *E. coli* GGT and human GGT by **2c**−**g** and **3** were fit to the first-order rate eq 1 to determine the observed pseudo-first-order rate constant for enzyme inactivation (k_{obs}) at each inhibitor concentration (see Experimental Procedures). With less reactive inhibitors, such as **2a** and **2b**, the inhibition of human GGT was so slow that the values of k_{obs} were determined by periodically measuring the remaining enzyme activity by incubating the enzyme with varying concentrations of the inhibitor without the substrate and by fitting the data to the

Table 1: Inhibitory Activities of **2a**−**g** and **3** toward *E. coli* and Human GGT

inhibitor	leaving group	pK_a[b]	k_{on}[a] (M^{-1} s^{-1}) *E. coli* GGT	k_{on}[a] (M^{-1} s^{-1}) human GGT
2a	*p*-OCH_3-C_6H_4OH	10.40	19 ± 1	0.16 ± 0.01
2b	*p*-CH_3-C_6H_4OH	10.21	24 ± 3	0.24 ± 0.03
2c	C_6H_4OH	9.98	120 ± 10	0.40 ± 0.03
2d	*p*-Cl−C_6H_4OH	9.41	610 ± 50	5.0 ± 0.2
2e	*p*-CF_3-C_6H_4OH	8.51	2900 ± 300	12 ± 1
2f	*p*-CN−C_6H_4OH	7.95	12000 ± 1000	46 ± 3
2g	*p*-NO_2-C_6H_4OH	7.15	35000 ± 3000	130 ± 10
3	4-UM[c]	8.10	16000 ± 1000	2400 ± 100
acivicin	HCl	−6.18	4200 ± 100[d]	0.40 ± 0.02[d]

[a] Second-order rate constant for enzyme inactivation. [b] pK_a of the leaving group. [c] 4-Methylumbelliferone. [d] Ref 38 (*38*).

first-order rate eq 4 (discontinuous assay). A plot of k_{obs} against inhibitor concentration gave a straight line without saturation until the highest inhibitor concentration under standard inhibition assay conditions, and the second-order rate constant for enzyme inactivation (k_{on}) was calculated according to eq 2 or 5. The values of k_{on} and pK_a of the leaving groups for **2a**−**g**, **3**, and acivicin are listed in Table 1.

The inhibition potency of the phosphonate diesters were more than 2 orders of magnitude larger than those of previously reported phosphonate monoesters **1a**−**d**. For example, phosphonates **2c**, **2e**, and **2f** inactivated *E. coli* GGT 40 to 460-times faster than the corresponding monoesters, under the same reaction conditions (*38*). The difference was even larger with human GGT: diesters **2e** and **2f** inactivated the human enzyme more than 380 times faster than monoesters **1b** and **1d** with the same leaving group, respectively. Even phosphonates **2a**−**c** with relatively poor leaving groups served as fairly good inhibitors of human GGT with activities almost comparable to that of acivicin, whereas monophenyl phosphonate **1a** failed to inactivate human GGT (*38*). These results are consistent with the higher electrophilicity of neutral phosphonate diesters compared to that of monoanionic phosphonates toward nucleophilic substitution (*40*) but may also be due to the higher affinity of the neutral phosphonates to the enzyme active site compared to that of the negatively charged phosphono monoesters. Keillor et al. reported that the affinity of APBA with rat GGT was significantly increased by decreasing the negative charge around the phosphorus at lower pH and postulated that electrostatic repulsion explained the result (*41*). The affinity of the phosphonate diesters also seemed to be affected by the steric bulk around the phosphorus because 2-amino-4-[butyl(phenyl)phosphono]butanoic acid, a butyl ester version of compound **2c** (Supporting Information), was a rather weak inhibitor of both *E. coli* and human GGT (k_{on} = 9.0 and 0.023 M^{-1} s^{-1}, respectively) than **2c**.

The phosphonate diesters were far more potent inhibitors toward *E. coli* GGT than toward the human enzyme: the inactivation rates of *E. coli* GGT by a series of *p*-substituted phenyl phosphonates **2a**−**g** were uniformly more than 2 orders of magnitude larger than those of human GGT. This also holds for the inhibition by phosphonate monoesters **1a**−**d**, where human GGT was inactivated much more slowly than the *E. coli* enzyme (*38*). Interestingly, phosphonate **3** with 4-methylumbelliferone as a leaving group showed an

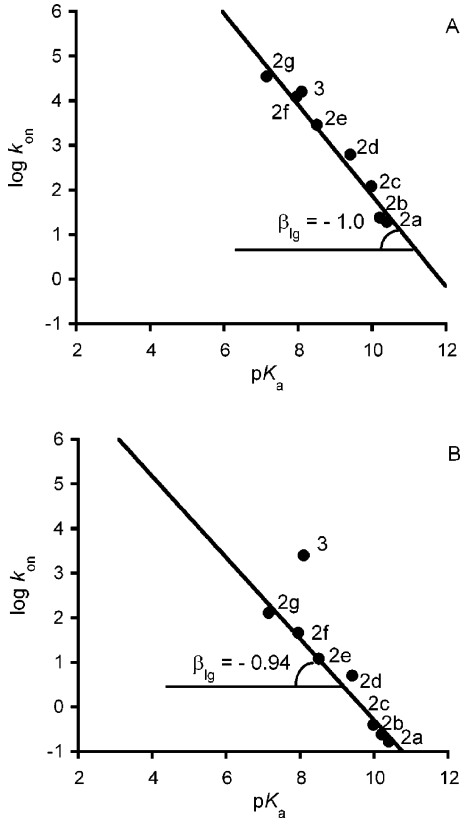

FIGURE 3: Brønsted plots relating the second-order rate constants for enzyme inactivation (k_{on}) with the leaving group ability for **2a**−**g** and **3**. (A) *E. coli* GGT. (B) Human GGT.

exceptionally strong activity toward human GGT (k_{on} = 2400 M^{-1} s^{-1}), but not toward *E. coli* GGT, in comparison with other phosphonates **2a**−**g**. As a result, compound **3** served as an extremely potent human GGT inhibitor with activity ca. 6000 times higher than that of acivicin. As far as we know, compound **3** was by far the most potent inhibitor of human GGT to date.

Another interesting facet regarding the properties of the phosphonate diesters is that the inactivation rate was highly dependent on the pK_a of the leaving group for both enzymes. Thus, the inhibition potency of phosphonate diesters **2a**−**g** and **3** toward *E. coli* and human GGTs increased significantly by increasing the leaving group ability of the phenols. For quantitative analysis of the substituent effect, Brønsted plots were constructed for the inactivation of *E. coli* and human GGTs by **2a**−**g** and **3**. A large negative slope (β_{lg} −1.0) with excellent linearity was obtained for the inactivation of *E. coli* GGT by phosphonate diesters **2a**−**g** and **3** (Figure 3A). Such a large leaving group dependence in phosphoryl transfer reactions (*50*) suggested that the reaction of the catalytic nucleophile of *E. coli* GGT and the electrophilic phosphorus of the phosphonate diesters proceeded via an anionic and dissociative transition state with substantial bond cleavage between the phosphorus and the leaving group as shown in Figure 4.

A similar negative slope (β_{lg} −0.94) with excellent linearity was also obtained for the inactivation of human GGT by phosphonate diesters **2a**−**g** (Figure 3B), suggesting that the phosphonylation of the active site of human GGT proceeded via a similar dissociative transition state. This is in sharp contrast to our previous results, where the inactivation rate of human GGT by phosphonate monoesters **1a**−**d**

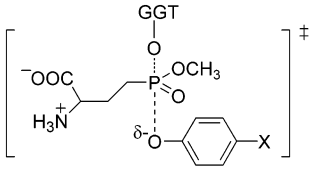

FIGURE 4: Transition state for the phosphonylation of the catalytic Thr residue by phosphonate diesters.

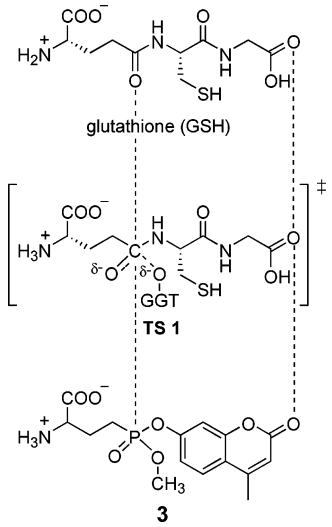

FIGURE 5: Structural comparison of phosphonate diester **3** with GSH and the proposed transition state for the hydrolysis of GSH.

was almost independent of the leaving group ability (*38*). The present results argue against the participation of a general acid catalysis in the phosphonylation of human GGT by phosphonate diesters **2a**−**g**.

Interestingly, the plot for compound **3** was located far above the line for **2a**−**g** with human GGT, whereas the plots of all of the phosphonates stood well on a line for the inactivation of the *E. coli* enzyme. This was indicative of a significantly higher activity of **3** than that expected from its leaving group ability toward human GGT: the observed inhibitory activity of **3** was ca. 100 times higher than that predicted from its leaving group ability (pK_a = 8.10). This might be attributed to the high affinity of **3** toward human GGT rather than its reactivity because the bimolecular reaction rate constant (k_{on}) is dependent on two kinetic parameters with respect to the reversible binding step of the inhibitor (K_i) and the unimolecular reaction rate constant (k_{inact}) for the formation of a covalent bond with the enzyme, as will be discussed later (see *Kinetics of Human GGT Inactivation by **5a** and **5b***). Thus, phosphonate diesters with a ligand that mimics the Cys−Gly moiety of glutathione might be well accommodated by the enzyme to increase inhibitory activity. Figure 5 shows the structure of **3** compared to those of glutathione and the proposed transition state for its hydrolysis (TS 1).

It is easily recognized that the carbonyl group of 4-methylumbelliferone in **3** is located nicely at the position occupied by the C-terminal carboxy group of glutathione and its transition state. Furthermore, the aromatic ring intervening between the phosphorus atom and the terminal carbonyl appears to mimic the planar amide bond of Cys−Gly. The preference of human GGT for **3** also seems related to the acceptor-site substrate specificity of mammalian GGT, where

Table 2: Inhibitory Activities of **4**, **5a**, and **5b** toward *E. coli* and Human GGT

		k_{on}[a] (M^{-1} s^{-1})	
inhibitor	pK_a[b]	*E. coli* GGT	human GGT
4	9.98	80 ± 2	75 ± 3
5a	9.71[c]	150 ± 10	51 ± 3
5b	9.84[c]	210 ± 10	0.33 ± 0.01

[a] Second-order rate constant for enzyme inactivation. [b] pK_a of the leaving group. [c] Calculated pK_a values of methyl 3-hydroxyphenylacetate (for **5a**) and methyl 4-hydroxyphenylacetate (for **5b**) using Advanced Chemistry Development (ACD/Labs) Software V8.14 for Solaris (1994−2006 ACD/Labs).

dipeptides with a C-terminal glycine carboxy group, such as Met−Gly, Ala−Gly, and Gly−Gly, are the preferred acceptor molecules (*25*).

*Design and Evaluation of Phosphonate Diesters **4**, **5a**, and **5b***. The significantly higher activity of **3** toward human GGT than those of simple phosphonate diesters **2a**−**g** suggested that the structures mimicking the Cys−Gly moiety of glutathione played an important role in the affinity of inhibitors to the active site of human GGT. We, therefore, designed phosphonate diesters **4**, **5a**, and **5b** for structure−activity relationships. Compound **4** is the closest analogue of the transition state (TS 1) for the hydrolysis of glutathione. Compound **5a** is an analogue of **3**, in which a highly acidic 4-methylumbelliferone (pK_a = 8.10) was replaced by a less acidic *m*-carboxymethylphenol but with a carboxy group at the position corresponding to the ring carbonyl of compound **3**. Compound **5b** with a *p*-CH_2COOH group was a reference compound of **5a** to see the effect of the position of the carboxy group on inhibitory activity.

The inactivation rates of *E. coli* and human GGT by **4**, **5a**, and **5b** are listed in Table 2. Despite the similar chemical reactivities of **4**, **5a**, and **5b** with that of **2c** as expected from their leaving group pK_a, phosphonates **4** and **5a** showed 188 and 128 times higher activity, respectively, than **2c** (k_{on} = 0.40 M^{-1} s^{-1}) toward human GGT. In contrast, the para-substituted phenyl phosphonate **5b** was a rather weak inhibitor of human GGT with activity comparable to that of **2c**. However, the *E. coli* enzyme was inactivated by **4**, **5a**, and **5b** with rates almost comparable with that of **2c** (k_{on} = 120 M^{-1} s^{-1}). The difference between *E. coli* and human GGTs as well as the difference among **4**, **5a**, and **5b** for the inactivation of human GGT was highlighted when the results were analyzed by Brønsted plots (Figure 6). For the inactivation of *E. coli* GGT, a plot for **4**, **5a**, and **5b** yielded the same line as those for **2a**−**g**. Even phosphonate **4**, the closest mimic of transition state 1, was not deviated at all from the line. For human GGT, however, a plot for **4** and **5a**, but not for **5b**, significantly deviated upward from the line for **2a**−**g**. Interestingly, a plot for **3**, **4**, and **5a** gave a new line (Figure 6B, dotted line) that was parallel to the line for **2a**−**g**, and the new line was almost superimposed on the line for the inactivation of *E. coli* GGT. These results indicated that the introduction of a carboxy or a carbonyl group in a specific position caused a dramatic increase in the inhibitory activity of the phosphonates toward human GGT, but not toward the *E. coli* enzyme, and that the activities of **3**, **4**, and **5a** toward human GGT approached those toward the *E. coli* enzyme. It is noteworthy that the

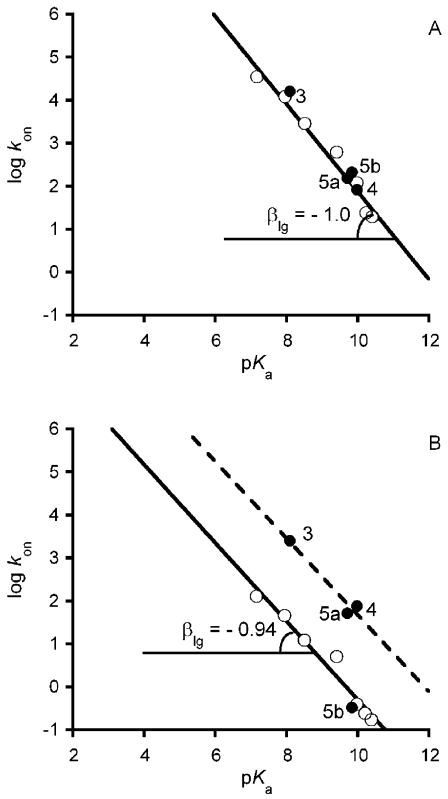

FIGURE 6: Brønsted plots relating the k_{on} values of **3**, **4**, **5a**, and **5b** (●) with the leaving group ability. The plots for **2a**−**g** are shown as open circles (○). (A) *E. coli* GGT. (B) Human GGT.

activity toward human GGT was increased by the same extent when a carboxy or a carbonyl group was introduced either in the leaving group (for **3** and **5a**) or in the remaining ligand (for **4**), provided that the functional group occupied the specific position topologically equivalent to the C-terminal carboxy group of the Cys−Gly moiety. These results cogently suggested that the 4-methylumbelliferyl, 2-hydroxybutyrylglycyl and *m*-carboxymethylphenyl moieties of **3**, **4**, and **5a**, respectively, mimicked the Cys−Gly moiety of glutathione in the transition state fairly well and occupied the Cys−Gly binding site of mammalian GGT when bound to the enzyme. The almost same level of the inhibitory activities of **4** and **5a** indicated that the side chain and amide linkage of the Cys−Gly moiety were reasonably mimicked by a simple phenyl ring of **5a** and that the terminal carboxy group was by far the most important recognition element by the human enzyme.

*Kinetics of Human GGT Inactivation by **5a** and **5b**.* It is rather interesting to know the reason for the more than 150 times higher activity of **5a** toward human GGT than that of structurally analogous **5b**. As described briefly in the previous section, the second-order rate constant for enzyme inactivation (k_{on}) is dependent on two kinetic parameters, K_i and k_{inact}, and is expressed as $k_{on} = k_{inact}/K_i$ according to the following kinetic mechanisms 1 and 2:

$$E + I \xrightarrow{k_{on}} E - I \qquad \text{(mechanism 1)}$$

$$E + I \overset{K_i}{\rightleftharpoons} E{\cdot}I \xrightarrow{k_{inact}} E - I \qquad \text{(mechanism 2)}$$

where K_i is the dissociation constant between the enzyme and the inhibitor before the formation of a covalent bond, and k_{inact} is the first-order rate constant for the formation of a covalent bond that results in enzyme inactivation. To gain insight into the molecular basis for the difference in the inhibitory activities, the kinetic parameters K_i and k_{inact} were determined separately for the inactivation of human GGT by **5a** and **5b** according to the kinetic mechanism 2. Because a plot of k_{obs} against inhibitor concentration usually gave a straight line without saturation under the standard inhibition assay conditions, the concentrations of **5a** and **5b** were increased until a saturation curve was obtained. The values of K_i and k_{inact} were calculated according to eq 3 (Experimental Procedures) and are summarized in Table 3. The K_i value for **5a** (0.17 mM) was significantly smaller than that for **5b** (7.2 mM), indicating that inhibitor **5a** was bound to the active site of human GGT more than 40 times as tightly as **5b** before the formation of a covalent bond. Furthermore, bound phosphonate **5a** reacted with the active-site nucleophile 4.2 times faster than **5b**, as estimated from the k_{inact} values.

Table 3: Kinetic Parameters for Human GGT Inactivation by **5a** and **5b**

inhibitor	K_i[a] (mM)	k_{inact}[a] (s^{-1})	k_{inact}/K_i ($M^{-1}\,s^{-1}$)	k_{on}[b] ($M^{-1}\,s^{-1}$)
5a	0.17	0.0097	57	51
5b	7.2	0.0023	0.32	0.33

[a] Calculated from eq 3 (Experimental Procedures). [b] Calculated from eq 2 (Experimental Procedures).

As a result, the calculated second-order rate constant for enzyme inactivation (k_{inact}/K_i) for **5a** was 178 times as large as that for **5b**, and the k_{inact}/K_i value for each inhibitor agreed well with the k_{on} value determined according to kinetic mechanism 1. These results clearly indicated that the significantly higher activity of **5a** toward human GGT was mainly due to improved affinity with the enzyme active site, while the increase in the phosphonylation rate (k_{inact}) also contributed to some extent (4.2 times). Therefore, the carboxymethyl function introduced at the meta position of the phenyl leaving group probably mimicked well the C-terminal carboxy group of the Cys−Gly moiety in the substrate and interacted specifically with the enzyme active site to improve the affinity of **5a**. The resulting productive binding of **5a** was also accompanied by the increase in the rate of active-site phosphonylation, thereby facilitating enzyme inactivation. In contrast, the carboxymethyl group at the para position (as in **5b**) failed to interact with the active site effectively. It is surprising that a small difference in the position of a carboxy group caused a large difference in the affinity of the inhibitors, but this is indicative of the highly specific recognition of human GGT for the Cys−Gly C-terminal carboxy group. A similar structure−activity relationship showing the importance of the terminal carboxy group was noted for the competitive inhibition of rat kidney GGT by a naturally occurring glutathione analogue. Anthglutin (L-γ-glutamyl-(*o*-carboxy)phenylhydrazide), originally isolated from the culture medium of *Penicillium oxalicum* (*52*), inhibited GGT with a K_i of 8.2 μM, whereas the para-substituted analogue, L-γ-glutamyl-(*p*-carboxy)-phenylhydrazide, served as a rather poor inhibitor (K_i = 800 μM) (*53*). The importance of the Cys−Gly moiety in the affinity of inhibitors was also reported with sulfur derivatives of L-Glu, in which the affinity of L-methionine sulfoxide was

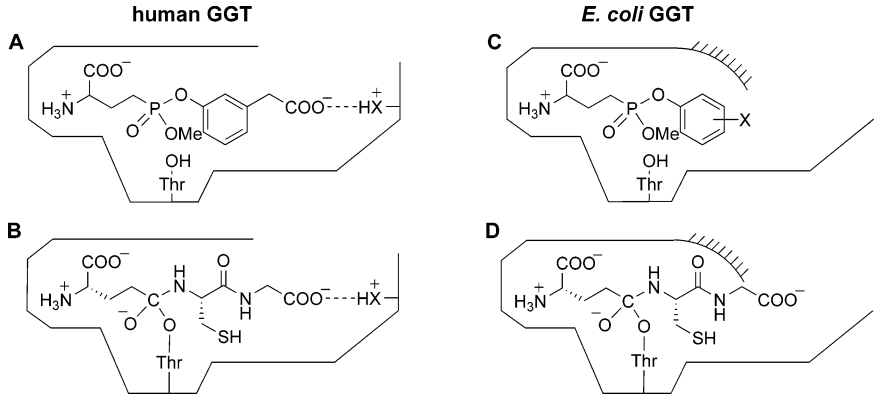

FIGURE 7: Schematic drawings of the active site of human GGT (A and B) and *E. coli* GGT (C and D) in complex with phosphonate diesters (A and C) and the tetrahedral intermediate for the hydrolysis of glutathione (B and D).

increased more than 100 times by substituting the *S*-methyl with a *S*-propionylglycine that mimicked Gly−Gly (*41*). Therefore, a single carboxy group can increase the activity of the inhibitors up to ca. 100 times, if it is introduced in a position that is topologically equivalent to the C-terminal carboxy group of the Cys−Gly moiety of the glutathione substrate. The significantly high activities of **3** and **4** can also be attributed to the improved affinities of these inhibitors with the active site by the recognition of the C-terminal carboxy group or the ring carbonyl group. In contrast, *E. coli* GGT was inactivated by a series of phosphonate diesters, including **4**, **5a**, and **5b** solely according to their chemical reactivity, irrespective of their structures. These results suggested that the *E. coli* enzyme had a rather broad substrate specificity to accommodate any phosphonate diesters almost equally without recognizing the C-terminal carboxy group.

Although the specificity of human GGT differed considerably from that of *E. coli* GGT, no significant difference was observed in the transition state for the phosphonylation of the catalytic residue (Figure 3, the Brønsted β_{lg} value of −0.94 vs −1.0) and in the inactivation rate by the most preferred phosphonate **4** (Table 2, k_{on} = 75 vs 80 M^{-1} s^{-1}). It seems, therefore, that human GGT was very similar to the *E. coli* enzyme in terms of the chemical reactivity with the phosphonates, the only difference being the active-site structure, which defines the specificity for the substrates as well as the phosphonate inhibitors. This notion raised the possibility of probing the active-site geometry of GGT by the phosphonates as transition-state analogue inhibitors.

Active-Site Geometries of GGT Probed by Transition State Analogue Inhibitors. GGT catalyzes the transfer of the γ-glutamyl group of γ-glutamyl donor substrates to a wide range of acceptor amino acids and peptides and exhibits a broad donor−substrate specificity for the moiety corresponding to the Cys residue of glutathione (*51*, *54*, *60*). This broad substrate specificity appears to be associated with the physiological roles of mammalian GGT: the enzyme metabolizes glutathione and its S-conjugates with a number of structurally diverse xenobiotics. Therefore, much research interest has focused on the donor- and acceptor-site substrate specificities of GGT for characterizing the enzyme from the view point of its biological function (*5*, *51*, *55*−*60*). Meister et al. extensively studied the substrate specificity of rat GGT and reported that the best acceptor molecules were L-cystine and aminoacylglycines, followed by glycyl amino acids and free amino acids (*51*, *60*). However, the acceptor substrates are thought to occupy the subsites for the Cys−Gly moiety of the donor substrate glutathione (*60*), and hence, the γ-glutamyl donor site partially overlaps the acceptor site. It has been observed that most acceptor substrates also act as inhibitors by competing with the donor substrates (*60*, *61*) and that GGT usually exhibits a significant autotranspeptidation activity at high substrate concentrations due to the binding of the donor substrate in the acceptor subsite (*60*). These catalytic properties of GGT have made the kinetic analysis rather complex (*25*, *60*). Besides, there are several potential problems in evaluating the affinity of substrates by kinetic parameters. For example, it has been pointed out that the apparent reactivity of the acceptor amino acids and peptides is highly dependent on the pK_a of the α-amino group that determines the effective concentration of the deprotonated form of amino acids and peptides as the true acceptor molecules (*63*). In addition, the apparent K_m value for γ-glutamyl donor substrates can be much smaller than the true Michaelis constant K_s because GGT catalyzes the reaction by a modified ping−pong mechanism via a γ-glutamyl enzyme intermediate with the deacylation as the rate-determining step (*26*, *64*).

The problems associated with kinetic analysis using true substrates can be avoided by using the kinetics of enzyme inactivation by phosphonates **2a**−**g**, **3**, **4**, and **5a** because phosphonates incorporate both the γ-glutamyl donor and acceptor moieties in their structure to mimic the transition state for the hydrolysis of γ-glutamyl donors (TS 1) or for the transpeptidation by amino acids and peptides (TS 2) as shown in Scheme 1. Hence, phosphonates serve as excellent chemical probes to gain insight into the active site geometries of GGT. The results of inhibition kinetics can be interpreted as unique active site geometries of human GGT. Thus, a hitherto unknown specific residue is present at the far end of the acceptor binding site, and this residue played a critical role in the recognition of the C-terminal carboxy group of glutathione and its S-conjugates in the transition state probably by hydrogen bonding and/or electrostatic interaction (Figure 7B). It has been suggested that there are three separate subsites corresponding to each amino acid component of glutathione in the active site of mammalian GGT (*65*). However, according to the results of active-site probing by phosphonate inhibitors, the cysteinyl side chain and the Cys−Gly amide linkage appeared to play a minor role in the recognition of the substrate. This seems reasonable from

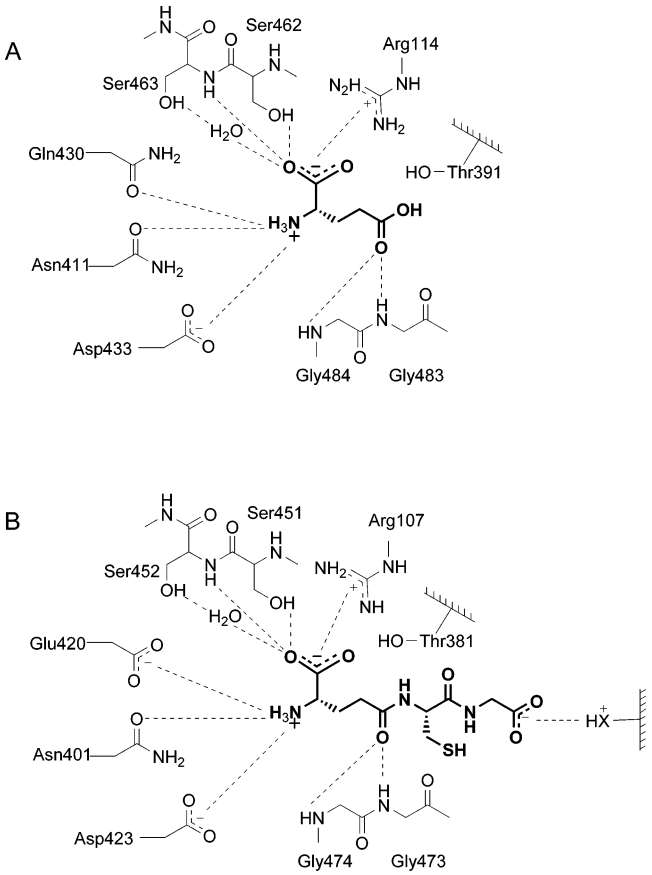

FIGURE 8: Schematic drawings of the glutamate binding site of GGT. (A) Active-site residues of *E. coli* GGT interacting with glutamate observed in the X-ray crystal structure (*66*). (B) Proposed interactions of the active-site residues of human GGT with glutathione.

the physiological function of mammalian GGT. Thus, mammalian GGT is responsible for the degradation of glutathione and its S-conjugates (*65*) and accommodates structurally diverse glutathione conjugates that are highly variable at the Cys side chain but are constant at the Cys−Gly amide bond and the C-terminal Gly carboxy group. This mode of substrate recognition is consistent with the reported substrate specificity of mammalian GGT, where cystine as well as dipeptides with a glycine C-terminal carboxy group, such as Met−Gly, Ala−Gly, Gln−Gly, Gly−Gly, served as far better acceptor substrates than monomeric amino acids (*25*). Cystine was probably bound in the acceptor site in an extended conformation so that the terminal α-carboxy group approached and interacted with the aforementioned key residue recognizing the C-terminal Cys−Gly carboxy group.

However, the *E. coli* enzyme was readily inactivated by any of the phosphonate diesters tested, and its inactivation rate correlated well with chemical reactivity but not with the structure of the phosphonates. Because the inhibitors used were substituted phenyl phosphonates and their derivatives, *E. coli* GGT may have tightly bound the phosphonates by recognizing the aromatic ring (Figure 7C). This is consistent with previous results that the aromatic amino acids were favored substrates of *E. coli* GGT as acceptor molecules (*5*). The *E. coli* enzyme accommodated the phosphonate diesters almost equally without recognizing the C-terminal carboxy group, suggesting that *E. coli* GGT lacked such a key residue recognizing the C-terminal Gly carboxy group as that anticipated in the human enzyme (Figure 7D).

Recently, the X-ray crystal structure of *E. coli* GGT was determined, and the detailed active-site residues of GGT at the γ-glutamyl site were identified for the first time (*66*). Figure 8A shows the active-site residues of *E. coli* GGT interacting with glutamate as observed in the X-ray crystal structure. Unfortunately, the attempts to identify the Cys−Gly binding site were not successful because of the rapid formation of the γ-glutamyl enzyme intermediate in the crystals of *E. coli* GGT in complex with glutathione (*66*). Hence, the Cys−Gly binding site of GGT still remains unidentified. So far, no crystal structure of mammalian GGT is available, but the residues essential for the recognition of the glutamate moiety are completely conserved in human GGT. Figure 8B depicts the proposed active-site residues of human GGT interacting with the glutamyl moiety and the proposed key residue recognizing the C-terminal Gly carboxy group of glutathione. The hitherto unknown Cys−Gly binding site might be identified by an X-ray structural analysis of *E. coli* GGT in complex with phosphonate inhibitor **4**, and this aspect of research is in progress in our collaborative study.

CONCLUSIONS

The electrophilic γ-phosphono diester analogues of glutamate served as highly potent transition-state analogue inhibitors of GGT that inactivated both bacterial and human enzymes in a mechanism-based manner. One such inhibitor (compound **3**) exhibited inhibitory activity more than 6000 times higher than that of acivicin and is the most potent inhibitor of human GGT to date. Enzyme inactivation proceeded probably by an initial reversible binding of the inhibitor (formation of the E−I complex), followed by phosphonylation of the active-site catalytic Thr residue (formation of the E−I dead end product) via a dissociative transition state. The inhibitors allowed the incorporation of a variety of leaving groups and Cys−Gly mimics at two sites of the γ-phosphono diester for use as chemical probes to gain insight into the active-site structures and the mechanism of substrate recognition of GGT. The human enzyme was highly selective and inactivated exceptionally rapidly by the phosphonates with a functional group that was chemically and topologically equivalent to the C-terminal carboxy group of substrate glutathione, but the *E. coli* enzyme was nonselective and was readily inactivated by any phosphonate diesters according to their chemical reactivities. These results suggested that a specific residue recognizing the C-terminal carboxy group of glutathione was present in the Cys−Gly binding site in human GGT, but not in the *E. coli* enzyme, and that this residue played a critical role in the recognition of glutathione and its S-conjugates by the human enzyme. Because mammalian GGTs are very similar to each other in primary sequences and conserved amino acids, this mode of substrate recognition appears to be a common characteristic of mammalian GGT and is deeply associated with its physiological function. Accordingly, the significantly different active-site structure of *E. coli* GGT suggested a biological role for bacterial GGT totally different from that of the mammalian enzymes (*67*, *68*). Furthermore, useful active-site probes could be developed by structural elaboration of the phosphonate diesters. For example, the derivatives

of compound **4** with a different side chain at the cysteinyl and/or the glycyl sites should be extremely effective in probing the acceptor-site substrate specificity with respect to the corresponding amino acid.

This study is a first step toward the development of highly selective GGT inhibitors that could be used *in vivo* as physiological probes and potential drug leads. GGT has been implicated in drug resistance (*11*−*13*, *18*, *69*), the metastatic activity (*15*−*17*) of cancer cells, and in many physiological disorders through glutathione homeostasis (*3*, *70*). An increasing number of epidemiological studies have shown that elevated serum GGT is associated with morbidity and mortality from cardiovascular disease (*24*, *71*) and with metabolic syndrome (*72*). A prooxidant effect of GGT (*73*−*75*) has attracted much research interest as a potential molecular mechanism for glutathione-driven lipid peroxidation and related physiological disorders such as atherosclerosis (*23*, *76*−*78*). However, the relationships between the diseases and the activity of GGT are still unclear because of a lack of sufficient experimental evidence. We believe, therefore, that the γ-phosphono diesters shown here should serve as useful physiological probes to unravel the currently mysterious relationships between the diseases and the activity of GGT, and may also lead to such drugs as those for increasing the efficacy of cancer chemotherapy and for treating cardiovascular diseases by modulating cellular glutathione metabolism and oxidative stress.

ACKNOWLEDGMENT

We thank Dr. Hideyuki Suzuki of the Graduate School of Biostudies, Kyoto University and Asahi Kasei Corporation for the generous gifts of purified *E. coli* GGT and human GGT HC-GTP (T-72), respectively.

SUPPORTING INFORMATION AVAILABLE

The synthesis of 2-amino-4-[butyl(phenyl)phosphono]-butanoic acid, the synthesis of 2-amino-4-[methyl(3-nitrophenyl)phosphono]butanoic acid, the inhibition of GGT by 2-amino-4-[butyl(phenyl)phosphono]butanoic acid, and the regain of activity of inactivated GGT. This material is available free of charge via the Internet at http://pubs.acs.org.

REFERENCES

1. Taniguchi, N., and Ikeda, Y. (1998) γ-Glutamyl transpeptidase: catalytic mechanism and gene expression, *Adv. Enzymol. Relat. Areas Mol. Biol. 72*, 239−278.
2. Hiratake, J., Suzuki, H., and Kumagai, H. (2004) γ-Glutamyl Transpeptidase and Its Precursor, in *Handbook of Proteolytic Enzymes* (Barrett, A. J., Rawlings, N. D., and Woessner, J. F., Eds.), 2nd ed., pp 2090−2094, Elsevier, Amsterdam, The Netherlands.
3. Whitfield, J. B. (2001) Gamma glutamyl transferase, *Crit. Rev. Clin. Lab. Sci. 38*, 263−355.
4. Hanigan, M. H., and Frierson, H. F., Jr. (1996) Immunohistochemical detection of gamma-glutamyl transpeptidase in normal human tissue, *J. Histochem. Cytochem. 44*, 1101−1108.
5. Suzuki, H., Kumagai, H., and Tochikura, T. (1986) γ-Glutamyltranspeptidase from *Escherichia coli* K-12: purification and properties, *J. Bacteriol. 168*, 1325−1331.
6. Hanigan, M. H., and Ricketts, W. A. (1993) Extracellular glutathione is a source of cysteine for cells that express γ-glutamyl transpeptidase, *Biochemistry 32*, 6302−6306.
7. Ruoso, P., and Hedley, D. W. (2004) Inhibition of γ-glutamyl transpeptidase activity decreases intracellular cysteine levels in cervical carcinoma, *Cancer Chemother. Pharmacol. 54*, 49−56.
8. Meister, A. (1991) Glutathione deficiency produced by inhibition of its synthesis, and its reversal; applications in research and therapy, *Pharmacol. Ther. 51*, 155−194.
9. de Saint Vincent, B. R., Mousset, S., and Jacquemin-Sablon, A. (1999) Cysteine control over glutathione homeostasis in Chinese hamster fibroblasts overexpressing a γ-glutamylcysteine synthease activity, *Eur. J. Biochem. 262*, 873−878.
10. Hanigan, M. H. (1995) Expression of gamma-glutamyl transpeptidase provides tumor cells with a selective growth advantage at physiologic concentrations of cyst(e)ine, *Carcinogenesis 16*, 181−185.
11. Godwin, A. K., Meister, A., O'Dwyer, P. J., Huang, C. S., Hamilton, T. C., and Anderson, M. E. (1992) High resistance to cisplatin in human ovarian cancer cell lines is associated with marked increase of glutathione synthesis, *Proc. Natl. Acad. Sci. U.S.A. 89*, 3070−3074.
12. Hanigan, M. H., Gallagher, B. C., Townsend, D. M., Gabarra, V. (1999) γ-Glutamyl transpeptidase accelerates tumor growth and increases the resistance of tumors to cisplatin *in vivo*, *Carcinogenesis 20*, 553−559.
13. Lewis, A. D., Hayes, J. D., and Wolf, C. R. (1988) Glutathione and glutathione-dependent enzymes in ovarian adenocarcinoma cell lines derived from a patient before and after the onset of drug resistance: intrinsic differences and cell cycle effects, *Carcinogenesis 9*, 1283−1287.
14. Hanigan, M. H., and Pitot, H. C. (1985) Gamma-glutamyl transpeptidase—its role in hepatocarcinogenesis, *Carcinogenesis 6*, 165−172.
15. Benlloch, M., Ortega, A., Ferrer, P., Segarra, R., Obrador, E., Asensi, M., Carretero, J., and Estrela, J. M. (2005) Acceleration of glutathione efflux and inhibition of γ-glutamyltranspeptidase sensitize metastatic B16 melanoma cells to endothelium-induced cytotoxicity, *J. Biol. Chem. 280*, 6950−6959.
16. Ortega, A. L., Carretero, J., Obrador, E., Gambini, J., Asensi, M., Rodilla, V., and Estrela, J. M. (2003) Tumor cytotoxicity by endothelial cells. Impairment of the mitochondrial system for glutathione uptake in mouse B16 melanoma cells that survive after *in vitro* interaction with the hepatic sinusoidal endothelium, *J. Biol. Chem. 278*, 13888−13897.
17. OBrador, E., Carretero, J., Ortega, A., Medina, I., Rodilla, V., Pellicer, J. A., and Estrela, J. M. (2002) γ-Glutamyl transpeptidase overexpression increases metastatic growth of B16 melanoma cells in the mouse liver, *Hepatology 35*, 74−81.
18. Pompella, A., De Tata, V., Paolicchi, A., and Zunino, F. (2006) Expression of γ-glutamyltransferase in cancer cells and its significance in drug resistance, *Biochem. Pharmacol. 71*, 231−238, and references cited therein.
19. Owen, A. D., Schapira, A. H., Jenner, P., and Marsden, C. D. (1996) Oxidative stress and Parkinson's disease, *Ann. N.Y. Acad. Sci. 786*, 217−223.
20. Sian, J., Dexter, D. T., Lees, A. J., Daniel, S., Jenner, P., and Marsden, C. D. (1994) Glutathione-related enzymes in brain in Parkinson's disease, *Ann. Neurol. 36*, 356−361.
21. Lee, D.-H., Ha, M.-H., Kim, J.-H., Christiani, D. C., Gross, M. D., Steffes, M., Blomhoff, R., and Jacobs, D. R. (2003) Gamma-glutamyltransferase and diabetes: a 4 year follow-up study, *Diabetologia 46*, 359−364.
22. Meisinger, C., Löwel, H., Heier, M., Schneider, A., and Thorand, B. (2005) Serum γ-glutamyltransferase and risk of type 2 diabetes mellitus in men and women from the general population, *J. Internal Med. 258*, 527−535.
23. Paolicchi, A., Minotti, G., Tonarelli, P., De Cesare, D., Mezzetti, A., Dominici, S., Comporti, M., and Pompella, A. (1999) γ-Glutamyl transpeptidase-dependent iron reduction and LDL oxidation—a potential mechanism in atherosclerosis, *J. Invest. Med. 47*, 151−160.
24. Ruttmann, E., Brant, L. J., Concin, H., Diem, G., Rapp, K., Ulmer, H., and the Vorarlberg Health Monitoring and Promotion Program Study Group (2005) γ-Glutamyltransferase as a risk factor for cardiovascular disease mortality: an epidemiological investigation in a cohort of 163,944 Austrian adults, *Circulation 112*, 2130−2137.
25. Allison, R. D. (1985) γ-Glutamyl transpeptidase: kinetics and mechanism, *Methods Enzymol. 113*, 419−437.
26. Keillor, J. W., Ménard, A., Castonguay, R., Lherbet, C., and Rivard, C. (2004) Pre-steady-state kinetic studies of rat kidney γ-glutamyl transpeptidase confirm its ping-pong mechanism, *J. Phys. Org. Chem. 17*, 529−536.

27. Gardell, S. J., and Tate, S. S. (1980) Affinity labeling of γ-glutamyl transpeptidase by glutamine antagonists. Effects of the γ-glutamyl transfer and proteinase activities, *FEBS Lett. 122*, 171−174.
28. Stole, E., Seddon, A. P., Wellner, D., and Meister, A. (1990) Identification of a highly reactive threonine residue at the active site of γ-glutamyl transpeptidase, *Proc. Natl. Acad. Sci. U.S.A. 87*, 1706−1709.
29. Smith, T. K., Ikeda, Y., Fujii, J., Taniguchi, N., and Meister, A. (1995) Different sites of acivicin binding and inactivation of γ-glutamyl transpeptidases, *Proc. Natl. Acad. Sci. U.S.A. 92*, 2360−2364.
30. Faribault, G., Wiebkin, P., Hamilton, J. W., Longnecker, D. S., and Curphey, T. J. (1987) γ-Glutamyltransferase activity in atypical acinar cell nodules of rat pancreas, *Toxicol. Appl. Pharmacol. 88*, 338−345.
31. Tate, S. S., and Meister, A. (1977) Affinity labeling of γ-glutamyl transpeptidase and location of the γ-glutamyl binding site on the light subunit, *Proc. Natl. Acad. Sci. U.S.A. 74*, 931−935.
32. Jayaram, H. N., Cooney, D. A., Ryan, J. A., Neil, G. L., Dion, R. L., and Bono, V. H. (1975) L-[α*S*, 5*S*]-α-amino-3-chloro-4,5-dihydro-5-isoxazoleacetic acid (NSC-163501): a new amino acid antibiotic with the properties of an antagonist of L-glutamine, *Cancer Chemother. Rep. 59*, 481−491.
33. Zalkin, H., and Smith, J. L. (1998) Enzymes utilizing glutamine as an amide donor, *Adv. Enzymol. Relat. Areas Mol. Biol. 72*, 87−144.
34. Earhart, R. H., and Neil, G. L. (1985) Acivicin in 1985, *Adv. Enz. Regul. 24*, 179−205.
35. Chittur, S. V., Klem, T. J., Shafer, C. M., and Jo Davisson, V. (2001) Mechanism for acivicin inactivation of triad glutamine amidotransferases, *Biochemistry 40*, 876−887.
36. Stein, R. L., DeCicco, C., Nelson, D., and Thomas, B. (2001) Slow-binding inhibition of γ-glutamyl transpeptidase by γ-boroGlu, *Biochemistry 40*, 5804−5811.
37. London, R. E., and Gabel, S. A. (2001) Development and evaluation of a boronate inhibitor of γ-glutamyl transpeptidase, *Arch. Biochem. Biophys. 385*, 250−258.
38. Han, L., Hiratake, J., Tachi, N., Suzuki, H., Kumagai. H., and Sakata, K. (2006) γ-(Monophenyl)phosphono glutamate analogues as mechanism-based inhibitors of γ-glutamyl transpeptidase, *Bioorg. Med. Chem. 14*, 6043−6054.
39. Inoue, M., Hiratake, J., Suzuki, H., Kumagai, H., and Sakata, S. (2000) Identification of catalytic nucleophile of *Escherichia coli* γ-glutamyltranspeptidase by γ-monofluorophosphono derivative of glutamic acid: N-terminal Thr-391 in small subunit is the nucleophile, *Biochemistry 39*, 7764−7771.
40. Behrman, E. J., Biallas, M. J., Brass, H. J., Edwards, J. O., and Isaks, M. (1970) Reactions of phosphonic acid esters with nucleophiles. I. Hydrolysis, *J. Org. Chem. 35*, 3063−3075.
41. Lherbet, C., and Keillor, J. W. (2004) Probing the stereochemistry of the active site of gamma-glutamyl transpeptidase using sulfur derivatives of L-glutamic acid, *Org. Biomol. Chem. 2*, 238−245.
42. Kosolapoff, G. M. (1948) Isomerization of alkyl phosphites. VII. Some derivatives of 2-bromoethane phosphonic acid, *J. Am. Chem. Soc. 70*, 1971−1972.
43. Chambers, J. R., and Isbell, A. F. (1964) A new synthesis of amino phosphonic acids, *J. Org. Chem. 29*, 832−836.
44. Laursen, B., Denieul, M.-P., and Skrydstrup, T. (2002) Formal total synthesis of the PKC inhibitor, balanol: preparation of the fully protected benzophenone fragment, *Tetrahedron 58*, 2231−2238.
45. Bradford, M. M. (1976) A rapid and sensitive method for the quantitation of microgram quantities of protein utilizing the principle of protein-dye binding, *Anal. Biochem. 72*, 248−254.
46. Smith, G. D., Ding, J. L., and Peters, T. J. (1979) A sensitive fluorimetric assay for γ-glutamyl transferase, *Anal. Biochem. 100*, 136−139.
47. Hosie, L., Sutton, L. D., and Quinn, D. M. (1987) *p*-Nitrophenyl and cholesteryl-*N*-alkyl carbamates as inhibitors of cholesterol esterase, *J. Biol. Chem. 262*, 260−264.
48. Hirschmann, R., Yager, K. M., Taylor, C. M., Witherington, J., Sprengeler, P. A., Phillips, B. W., Moore, W., and Smith, A. B., III. (1997) Phosphonate diester and phosphonamide synthesis. Reaction coordinate analysis by ^{31}P NMR spectroscopy: identification of pyrophosphonate anhydrides and highly reactive phosphonylammonium salts, *J. Am. Chem. Soc. 119*, 8177−8190.
49. Tsuji, T., Kataoka, T., Yoshioka, M., Sendo, Y., Nishitani, Y., Hirai, S., Maeda, T., and Nagata, W. (1979) Synthetic studies on β-lactam antibiotics. VII. Mild removal of the benzyl ester protecting group with aluminum trichloride, *Tetrahedron Lett. 30*, 2793−2796.
50. Hengge, A. C., and Onyido, I. (2005) Physical organic perspectives on phospho group transfer from phosphates and phosphinates, *Curr. Org. Chem. 9*, 61−74.
51. Tate, S. S., and Meister, A. (1974) Interaction of γ-glutamyl transpeptidase with amino acids, dipeptides, and derivatives and analogs of glutathione, *J. Biol. Chem. 249*, 7593−7602.
52. Minato, S. (1979) Isolation of anthglutin, an inhibitor of γ-glutamyl transpeptidase from *Penicillium oxalicum*, *Arch. Biochem. Biophys. 192*, 235−240.
53. Griffith, O. W., and Meister, A. (1979) Translocation of intracellular glutathione to membrane-bound γ-glutamyl transpeptidase as a discrete step in the γ-glutamyl cycle: glutathionuria after inhibition of transpeptidase, *Proc. Natl. Acad. Sci. U.S.A. 76*, 268−272.
54. Tate, S. S., and Ross, M. E. (1977) Human kidney γ-glutamyl transpeptidase. Catalytic properties, subunit structure, and localization of the γ-glutamyl binding site on the light subunit, *J Biol. Chem. 252*, 6042−6045.
55. Thompson, G. A., and Meister, A. (1976) Hydrolysis and transfer reactions catalyzed by γ-glutamyl transpeptidase; evidence for separate substrate sites and for high affinity of L-cystine, *Biochem. Biophys. Res. Commun. 71*, 32−36.
56. Cook, N. D., Upperton, K. P., Challis, B. C., and Peters, T. J. (1987) The donor specificity and kinetics of the hydrolysis reaction of γ-glutamyltransferase. *Biochim. Biophys. Acta 914*, 240−245.
57. Cook, N. D., and Peters, T. J. (1985) Purification of γ-glutamyltransferase by phenyl boronate affinity chromatography. Studies on the acceptor specificity of transpeptidation by rat kidney γ-glutamyltransferase, *Biochim. Biophys. Acta 828*, 205−212.
58. Cornwell, P. D., and Watkins, J. B., III. (2001) Changes in the kinetic parameters of hepatic γ-glutamyltransferase from streptozotocin-induced diabetic rats, *Biochim. Biophys. Acta 1545*, 184−191.
59. Meredith, M. J. (1991) Variations in γ-glutamyl transpeptidase glycosylation and kinetic parameters in cultured liver cells, *Biochem. Int. 25*, 321−330.
60. Thompson, G. A., and Meister, A. L. (1977) Interrelationships between the binding sites for amino acids, dipeptides, and γ-glutamyl donors in γ-glutamyl transpeptidase, *J. Biol. Chem. 252*, 6792−6798.
61. McIntyre, T. M., and Curthoys, N. P. (1979) Comparison of the hydrolytic and transfer activities of rat renal γ-glutamyltranspeptidase, *J. Biol. Chem. 254*, 6499−6504.
62. Abbott, W. A., Griffith, O. W., and Meister, A. (1986) Gamma-glutamyl-glutathione. Natural occurrence and enzymology, *J. Biol. Chem. 261*, 13657−13661.
63. Cook, N. D., and Peters, T. J. (1985) The effect of pH on the transpeptidation and hydrolytic reactions of rat kidney gamma-glutamyltransferase, *Biochim. Biophys. Acta 832*, 142−147.
64. Walsh, C. (1979) *Enzymatic Reaction Mechanism*, pp 64−82, W. H. Freeman and Co., San Francisco, CA.
65. Tate, S. S., and Meister, A. (1985) γ-Glutamyl transpeptidase from kidney, *Methods Enzymol. 113*, 400−419.
66. Okada, T., Suzuki, H., Wada, K., Kumagai, H., and Fukuyama, K. (2006) Crystal structures of γ-glutamyltranspeptidase from *Escherichia coli*, a key enzyme in glutathione metabolism, and its reaction intermediate, *Proc. Natl. Acad. Sci. U.S.A. 103*, 6471−6476.
67. Robins, R., and Davies, D. (1981) The role of glutathione in amino-acid absorption, *Biochem. J. 194*, 63−70.
68. Suzuki, H., Hashimoto, W., and Kumagai, H. (1993) *Escherichia coli* K-12 can utilize an exogenous γ-glutamyl peptide as an amino acid source, for which γ-glutamyltranspeptidase is essential, *J. Bacteriol. 175*, 6038−6040.
69. Karp, D. R., Shimooku, K., and Lipsky, P. E., (2001) Expression of γ-glutamyl transpeptidase protects ramos B cells from oxidation-induced cell death, *J. Biol. Chem. 276*, 3798−3804.
70. Dalton, T. P., Chen, Y., Schneider, S. N., Nebert, D. W., and Shertzer, H. G. (2004) Genetically altered mice to evaluate glutathione homeostasis in health and disease, *Free Radical Biol. Med. 37*, 1511−1526.
71. Lee, D. H., Silventoinen, K., Hu, G., Jacobs, D. R., Jr., Jousilahti, P., Sundvall, J., and Tuomilehto, J. (2006) Serum γ-glutamyltransferase predicts non-fatal myocardial infarction and fatal

coronary heart disease among 28838 middle-aged men and women, *Eur. Heart J. 27*, 2170−2176.
72. Nakanishi, N., Suzuki, K., and Tatara, K. (2004) Serum γ-glutamyltransferase and risk of metabolic syndrome and type 2 diabetes in middle-aged Japanese men, *Diabetes Care 27*, 1427−1432.
73. Stark, A.-A., Zeiger, E., and Pagano, D. A. (1993) Glutathione metabolism by γ-glutamyltranspeptidase leads to lipid peroxidation: characterization of the system and relevance to hepatocarcinogenesis, *Carcinogenesis 14*, 183−189.
74. Dominici, S., Paolicchi, A., Lorenzini, E., Maellaro, E., Comporti, M., Pieri, L., Minotti, G., and Pompella, A. (2003) γ-Glutamyltransferase-dependent prooxidant reactions: A factor in multiple processes, *BioFactors 17*, 187−198.
75. Dominici, S., Paolicchi, A., Corti, A., Maellaro, E., and Pompella, A. (2005) Prooxidant reactions promoted by soluble and cell-bound γ-glutamyltransferase activity, *Methods Enzymol. 401*, 484−501.
76. Pompella, A., Emdin, M., Passino, C., and Paolicchi, A. (2004) The significance of serum γ-glutamyltransferase in cardiovascular diseases, *Clin. Chem. Lab. Med. 42*, 1085−1091.
77. Emdin, M., Pompella, A., and Paolicchi, A. (2005) γ-Glutamyltransferase, atherosclerosis, and cardiovascular disease: triggering oxidative stress within the plaque, *Circulation 112*, 2078−2080.
78. Paolicchi, A., Emdin, M., Passino, C., Lorenzini, E., Titta, F., Marchi, S., Malvaldi, G., and Pompella, A. (2006) β-Lipoprotein- and LDL-associated serum γ-glutamyltransferase in patients with coronary atherosclerosis. *Atherosclerosis 186*, 80−85.

BI061890J